Empa
Überlandstrasse 129
CH-8600 Dübendorf
T +41 58 765 11 11
F +41 58 765 11 22
www.empa.ch

Materials Science & Technology

Bundesamt für Umwelt BAFU
Abteilung Lärm und NIS
z. Hd. Herr Franz Kuster
3003 Bern

Rail Track Noise Emission: Influence of Under Sleeper Pads on Railway Rolling Noise Emissions

Im Auftrag der Schweizerischen Eidgenossenschaft

Untersuchungsbericht:	Empa-Nr. 5211.01578.100.01
Ihr Auftrag vom:	26. September 2018
Anzahl Seiten inkl. Beilagen:	18

Inhaltsverzeichnis

Dübendorf, 08. Oktober 2019	Abteilung Akustik / Lärmminderung
Der Projektleiter:	Der Abteilungsleiter:
Dr. Benjamin Morin	Dr. Jean-Marc Wunderli

Anmerkung: Bericht und Unterlagen werden 10 Jahre archiviert.

Appendix

Impressum

Auftraggeber:	Schweizerische Eidgenossenschaft; Bundesämter für Umwelt (BAFU) und Verkehr (BAV); CH-3003 Bern. Das BAFU und das BAV sind Ämter des Eidg. Departements für Umwelt, Verkehr, Energie und Kommunikation (UVEK)
Auftragnehmer:	Empa
Autor/Autorin:	Benjamin Morin, Armin Zemp
Begleitung BAFU/	Franz Kuster, Fredy Fischer
BAV:	Robert Attinger, Christoph Dürig
Hinweis:	Dieser Bericht wurde im Auftrag der Bundesämter für Umwelt (BAFU) und Verkehr (BAV) verfasst. Für den Inhalt ist alleine der Auftragnehmer verantwortlich.

Introduction

This report is the final contribution to the ''Rail Track Noise Emission: Influence of Under Sleeper Pads on Railway Rolling Noise Emissions'' project. The first section is a short reminder about the analytical model developed for the project and described in previous reports and also presents its validation with measurements. The second part uses this model to perform an assessment of the influence of the USP elastic and damping properties separately. In the third section, a direct application of the analytical model to real life USP is done by comparing the performance of three pads selected by SBB. The last and fourth section is about the influence of the temperature during measurements, especially when comparing the performance of the track with or without pads.

To conclude this reports, a set of guidelines are given on the use of USP as well as an update of the budget and of the project modules.

1 Analytical track model

The model is based on the state of art [1] approach of modelling the rails as infinite beams and the rest of the track as continuous or discrete spring supports. Many improvements compared to the state of art were implemented following Module 2 to 4 of the project. The final model is described as follow:

- For the vertical direction, the rail is represented by an infinite beam, discretely supported. Each support is composed of a spring for the rail pad and a finite beam for the sleeper. The sleeper itself is continuously supported by an elastic layer accounting for the USP and the ballast.
- For the horizontal direction, the rail is represented by a 3 beams model, allowing for bending and torsion, and the support is discrete. Each support is composed of a spring for the rail pad and a finite beam for the sleeper. The sleeper itself is continuously supported by an elastic layer accounting for the USP and the ballast.

In the present version, the vertical model represent a simplification of the work from [2] were the rail is represented as a beam instead of using Finite Elements. For the horizontal direction, the present version of the model is an extension of the work from [3] were only a continuous support is used.

The vertical and horizontal models are validated by comparison with the Effretikon measurements performed by Empa in November 2018. For the vertical direction, the measured Track Decay Rate (Figure 1) is available and is used as a reference. For the horizontal direction, only the track dynamic is available so the point accelerance (acceleration transfer function at the excitation location) is used as the reference (Figure 2). As the Track Decay Rates and acoustic Sound Power Levels presented later are calculated directly from the track transfer functions, the validation of the horizontal model with the transfer functions is sufficient even if no measured TDR is available.
The horizontal model (Figure 2) shows a very good agreement with the measurements. The levels of both measurements and model predictions are the same and only a slight shift in frequency is happening at the peaks captured by the model. The main difference occurs at around 400 Hz where the model over-estimates the track response.
For the vertical model (Figure 1) the comparison is slightly worse than in the horizontal direction: the shift in frequency is larger and the level values are over-estimated at very-low and very-high frequencies. This difference is due to the simpler nature of the rail model: in the vertical case only a single beam is used instead of three for the horizontal case. Because of that some behaviour of the rail, like foot flapping, are absent from the simulation and cause a deviation from the measurements. However the overall levels and frequency content of the simulation are very close from the measurements and the vertical model can be used in its present form.

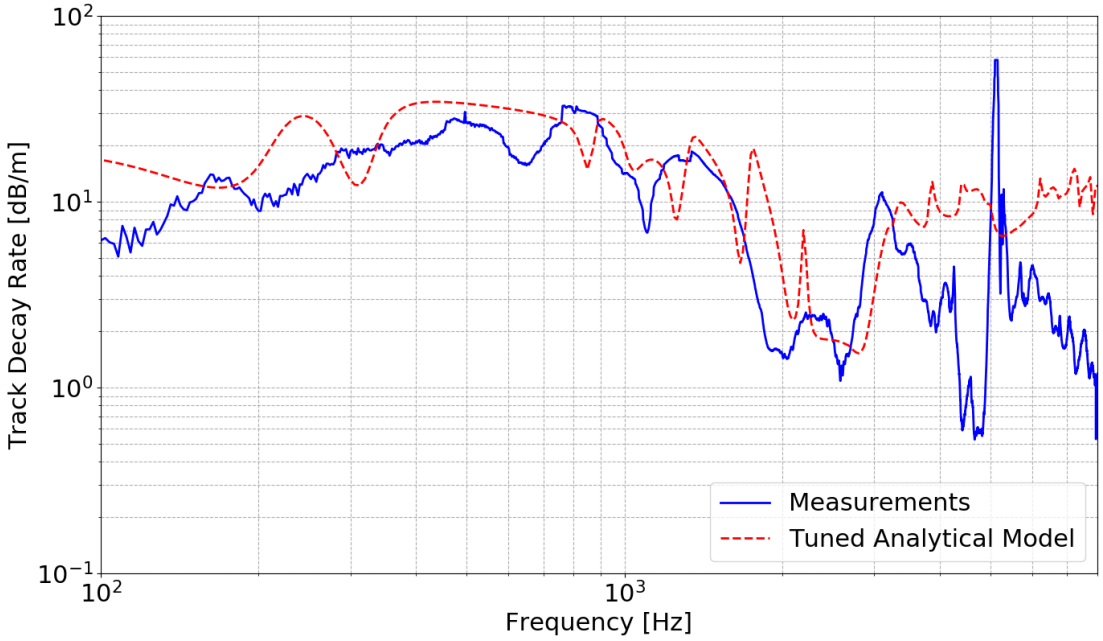

Figure 1 – Validation of the vertical analytical track model

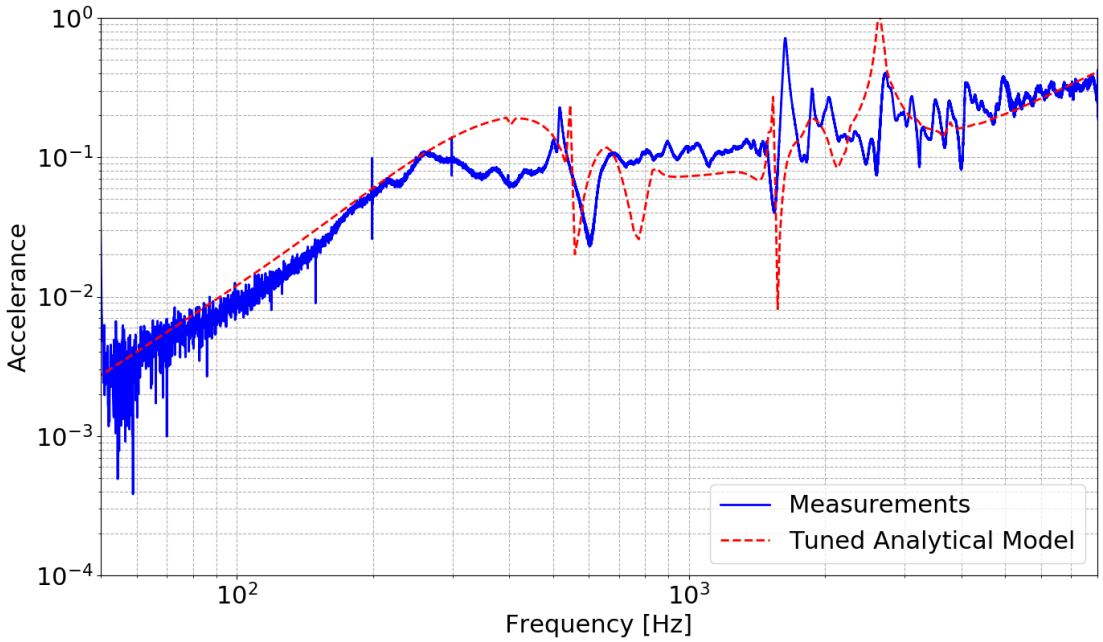

Figure 2 – Validation of the lateral analytical track model

2 Assessment of the USP influence on the track acoustics

Using the models previously presented, a parametric study is here conducted to estimate the influence of the USP properties on the dynamics and acoustic response of the track.
For the dynamics, the Track Decay Rates are presented. Their calculation relies on the track transfer functions. For the acoustics, the Sound Power Levels are presented. Their calculation is done following [1] and also rely on the track transfer functions.
Figures (3) and (4) show the influence of the USP stiffness in the vertical direction.
Figures (5) and (6) show the influence of the USP loss factor in the vertical direction.
Figures (7) and (8) show the influence of the USP stiffness in the lateral direction.
Figures (9) and (10) show the influence of the USP loss factor in the lateral direction.

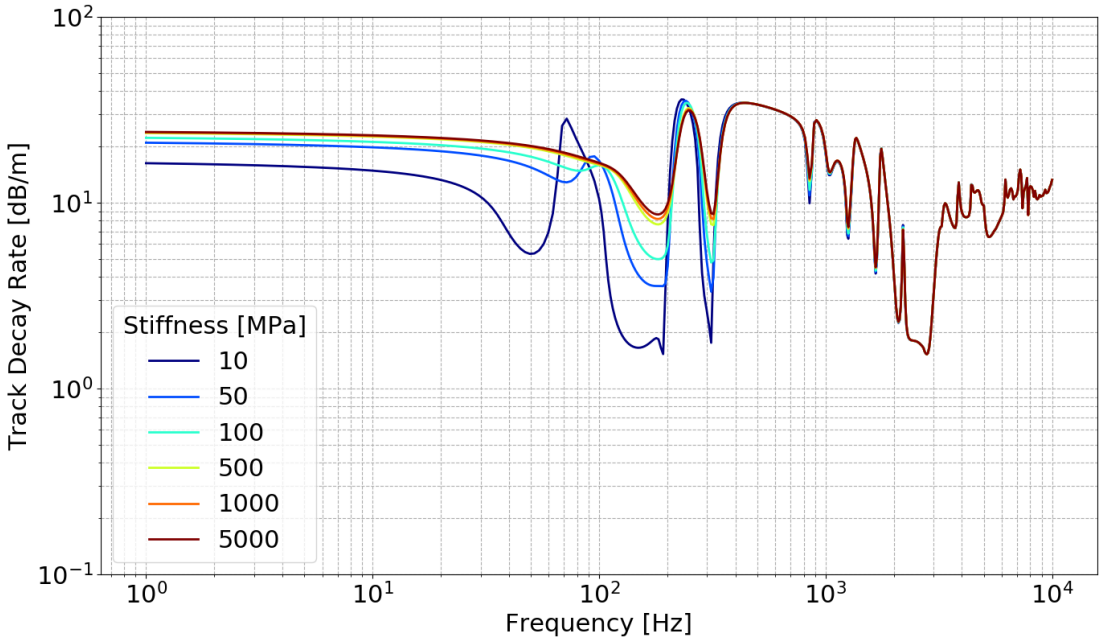

Figure 3 – Influence of the USP stiffness on the vertical TDR

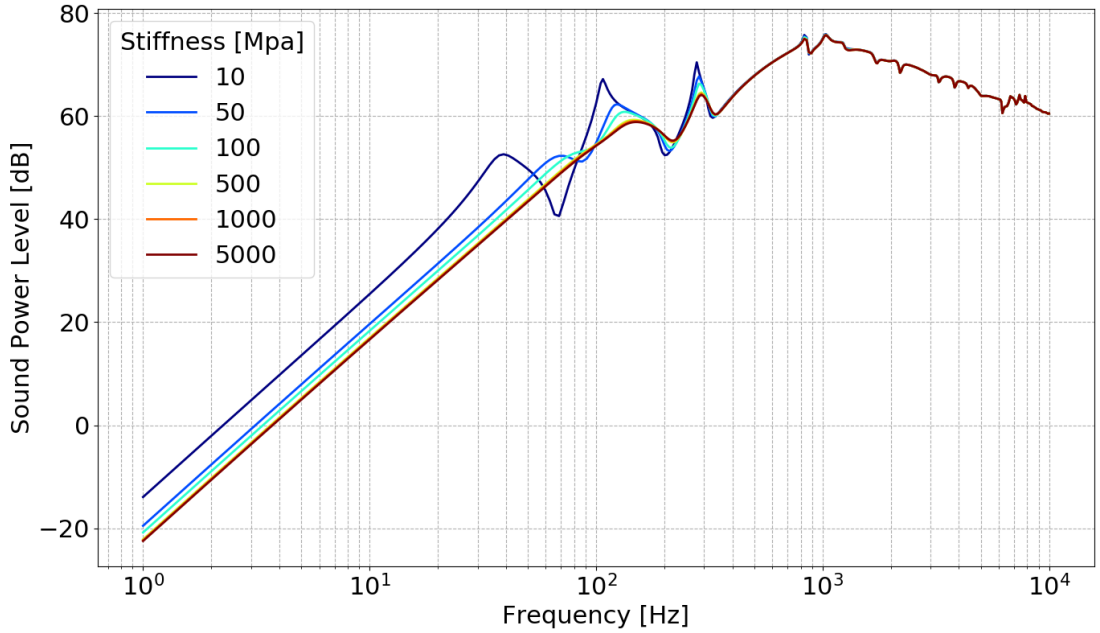

Figure 4 – Influence of the USP stiffness on the vertical Sound Power Levels

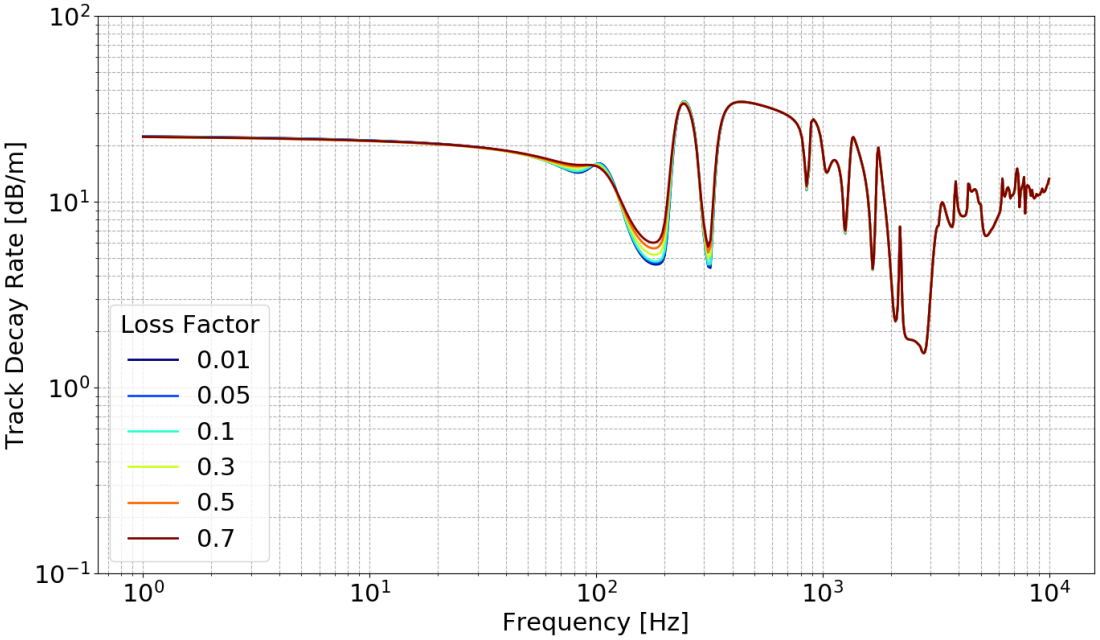

Figure 5 – Influence of the USP loss factor on the vertical TDR

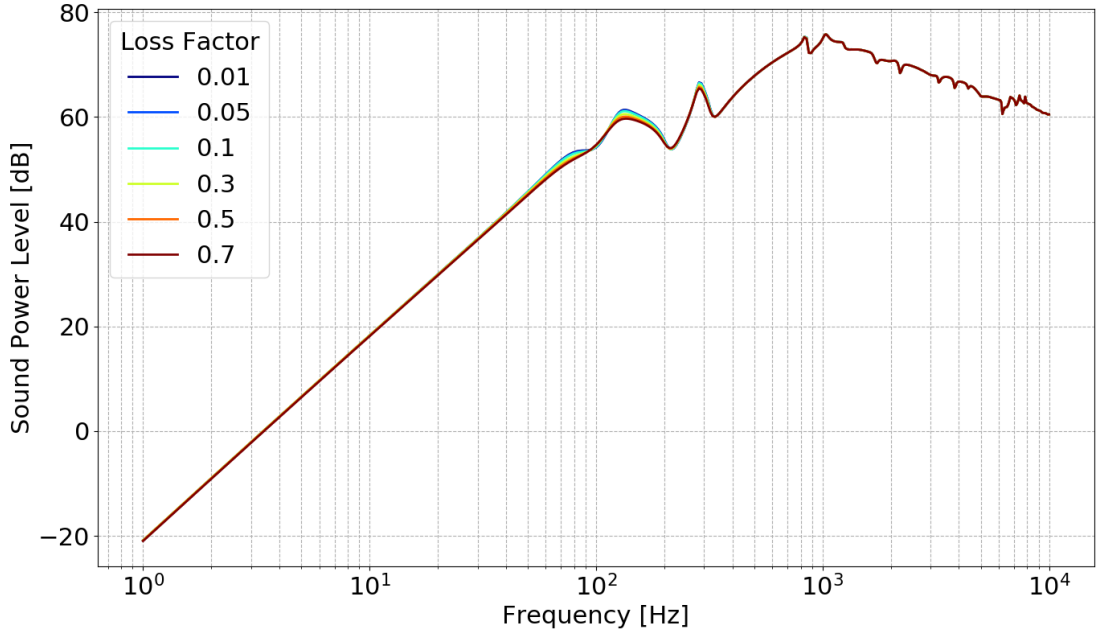

Figure 6 – Influence of the USP loss factor on the vertical Sound Power Levels

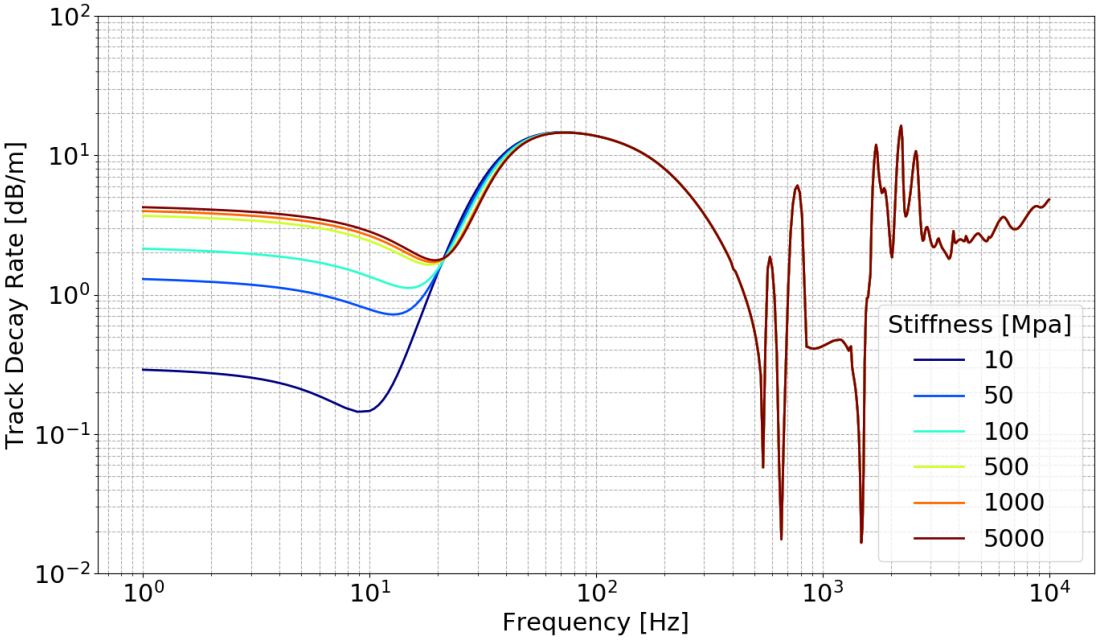

Figure 7 – Influence of the USP stiffness on the lateral TDR

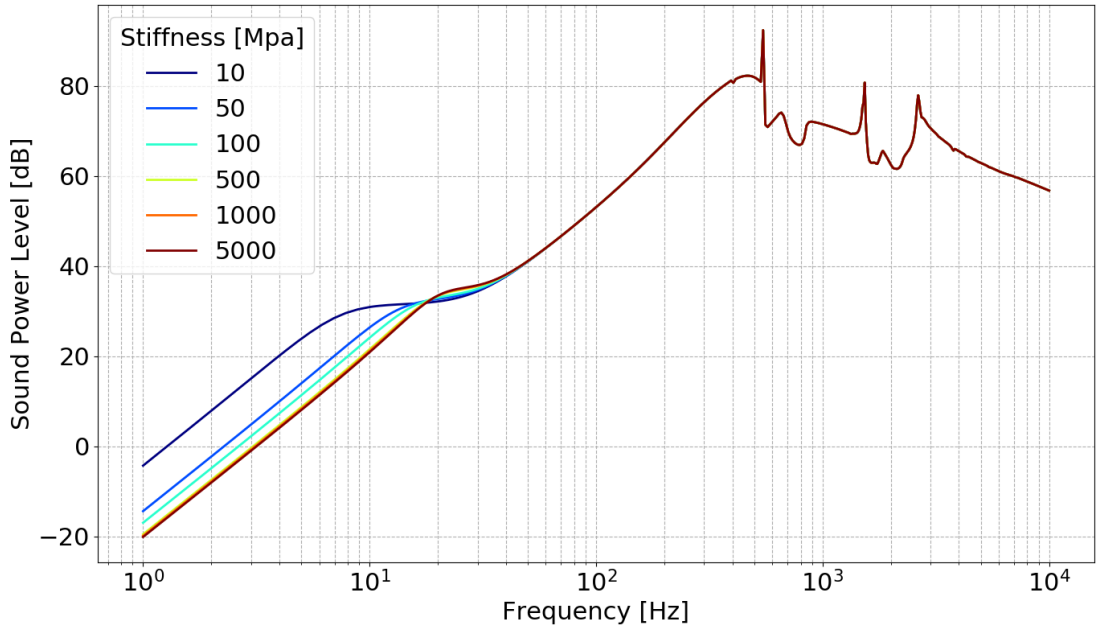

Figure 8 – Influence of the USP stiffness on the lateral Sound Power Levels

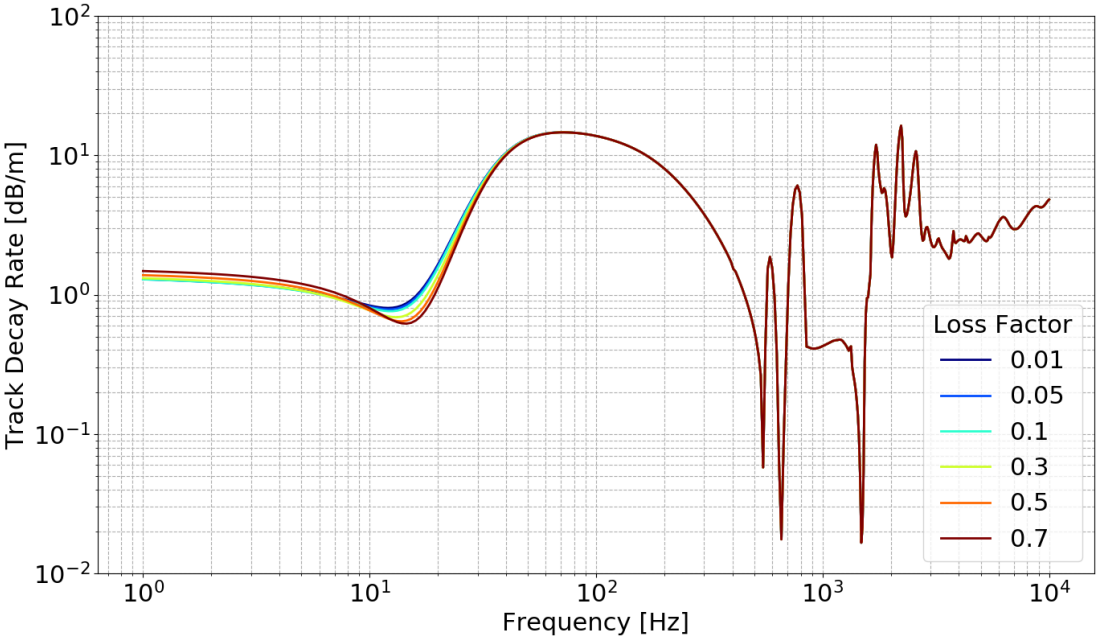

Figure 9 – Influence of the USP stiffness on the lateral TDR

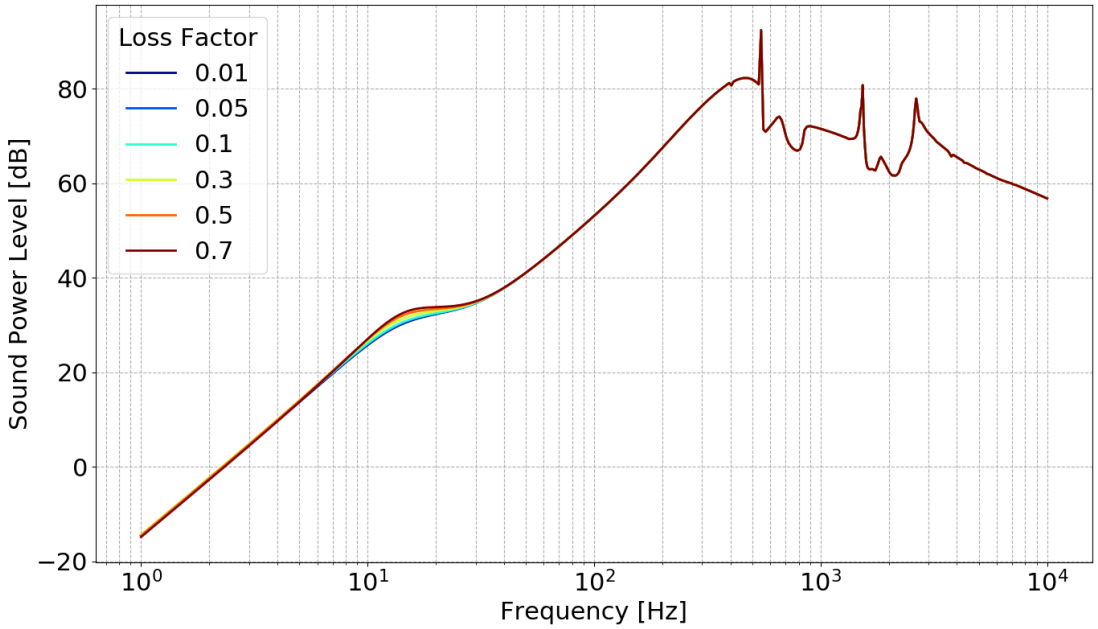

Figure 10 – Influence of the USP loss factor on the lateral Sound Power Levels

The conclusions of the parametric study are the following:

- In the lateral direction the USP influence is limited to very low frequencies, up to a few dozen Hz. In the vertical direction the USP influence is limited to low frequencies, up to a few hundred Hz.
- Both, for vertical or horizontal directions, the USP stiffness is the most important factor for noise emission. The stiffer the pad the lower the noise emission.
- The loss factor is almost irrelevant. This is due to fact that the damping from the ballast is already very high.
- The stiffness values used here are chosen on purpose to be rather extreme, thus making the influence on the track response more explicit. In reality, when choosing between different models of USP from manufacturers, the difference between pads will be much lower.

3 Application to real USP

The analytical model is here applied to the case of three USP from Getzner, selected by SBB: the SLN1510 (soft pad), SLB2210 (medium) and SLB3007 (hard). The sound power level emitted is given in Figure 11 for a lateral excitation and in Figure 12 for a vertical excitation.
For a lateral excitation, the softer pad results in a maximum of 15 dB increase while the harder pad results in a maximum of 8 dB, both compared to a track without USP.
For a vertical excitation, the softer pad results in a maximum of 4 dB increase while the harder pad results in a maximum of 1 to 2 dB. These increases in noise emission are however limited to very low frequencies: up to 30 Hz for the lateral case and up to 300 Hz for the vertical one, only a small fraction of the acoustic range.

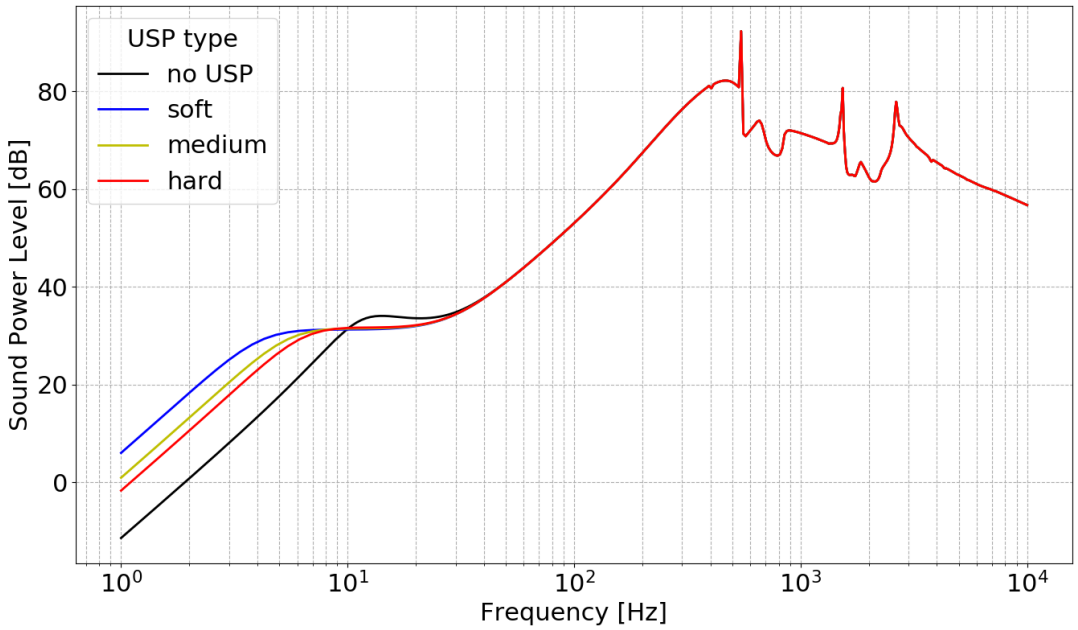

Figure 11 – Acoustic performance of the selected pads for a lateral excitation

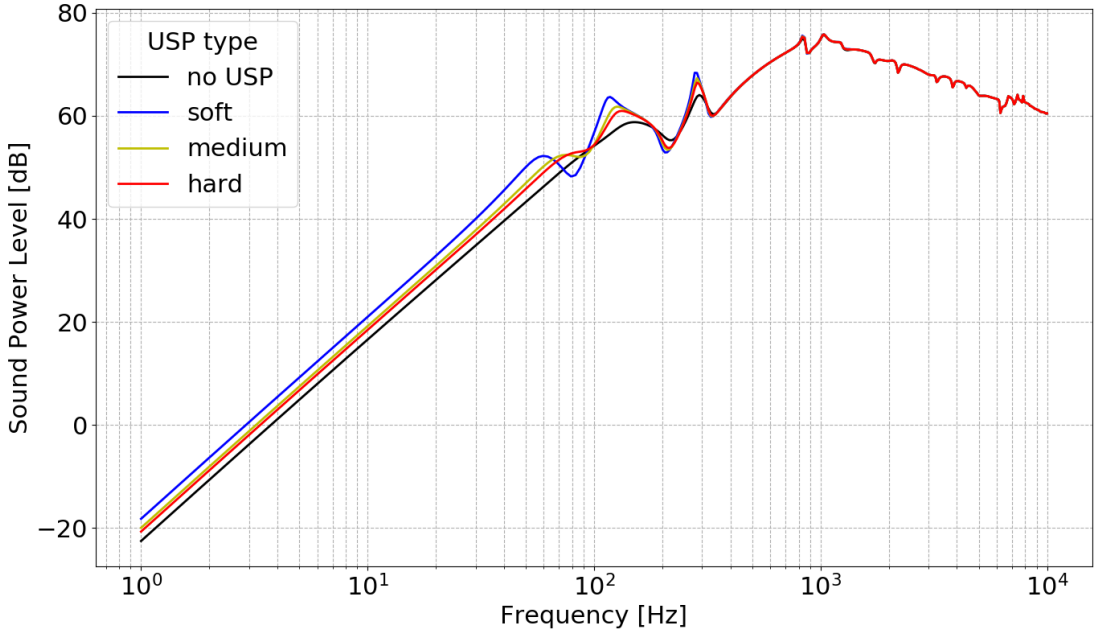

Figure 12 – Acoustic performance of the selected pads for a vertical excitation

4 Influence of the temperature

The poly-urethane foam, from which the selected USPs are made, is a temperature dependent material that stiffens with decreasing temperatures. This may be important in countries like Switzerland where, depending on the season and location of the track, various temperature conditions can be encountered.
In Figure 13, the DMA measurements of the SLB3007 material are used to derive its storage modulus master curves at -10°C and 20°C. As expected, the lower temperature is linked to a high modulus (stiffer material), and the increase is of one order of magnitude (10x).

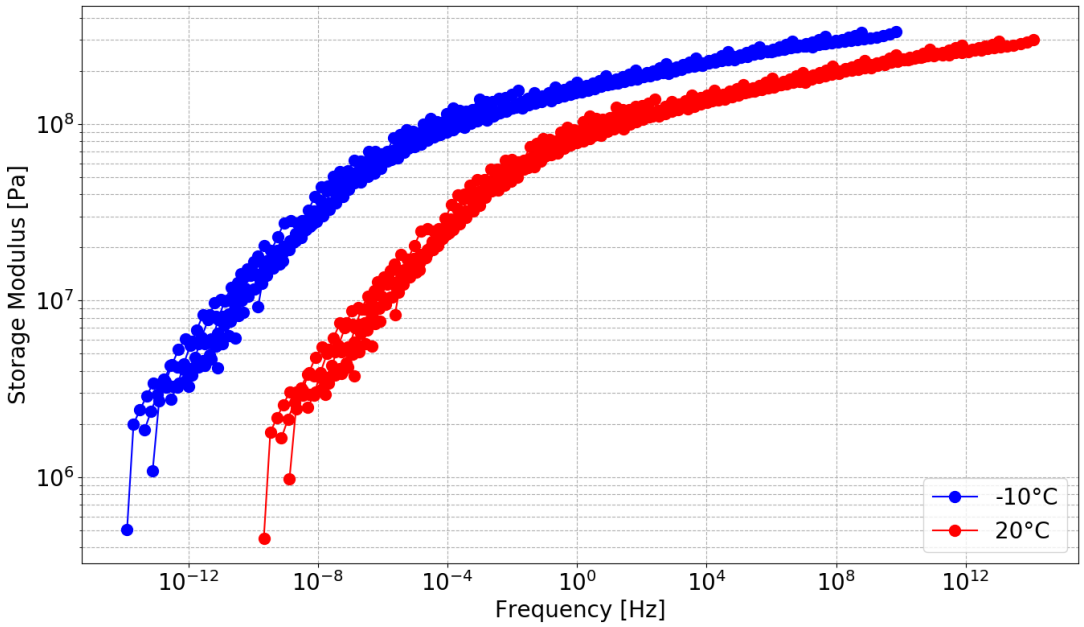

Figure 13 – Storage modulus of the SLB3007 material at -10°C and 20°C

The pad properties at both temperatures are derived from this two curves following the super-element technique presented in the 6 months report and then injected in the analytical model to estimate the effects on the noise emission for a lateral excitation (Figure 14) and for a vertical excitation (Figure 15).
The low temperature decreases the sound power level by 8 dB for the lateral case and by 2 dB for the vertical case. Again these effects are limited to very low frequency ranges.
In the context of testing USPs in-situ, efforts should be made to measure both the reference track and the track with USPs during the same period of the year, if possible on the same day and at two close locations.

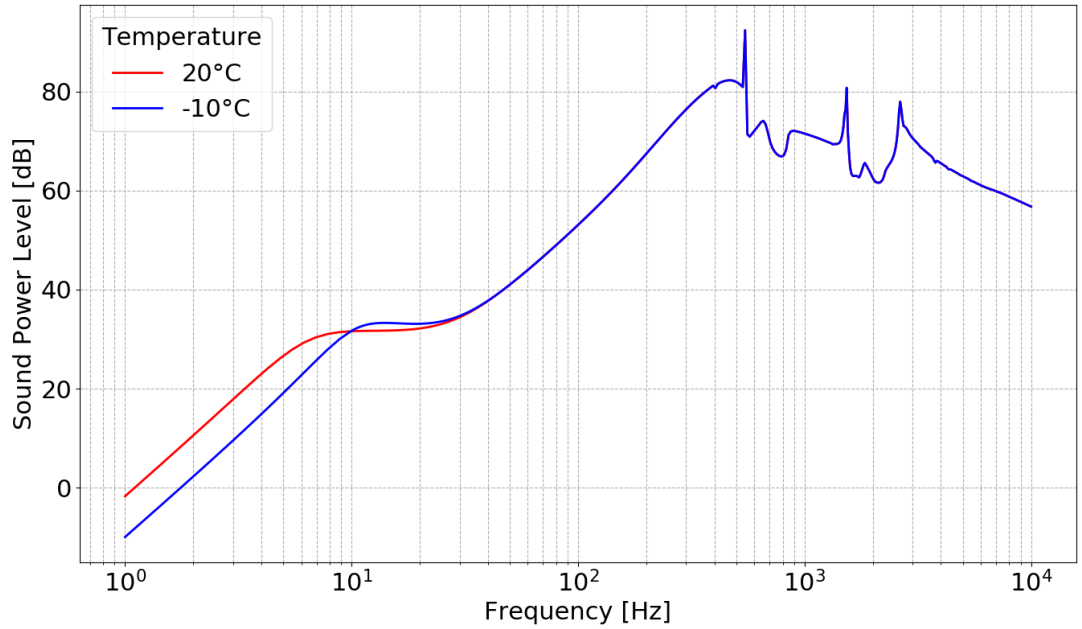

Figure 14 – Effect of the temperature on the acoustic performance of the SLB3007 USP for a lateral excitation

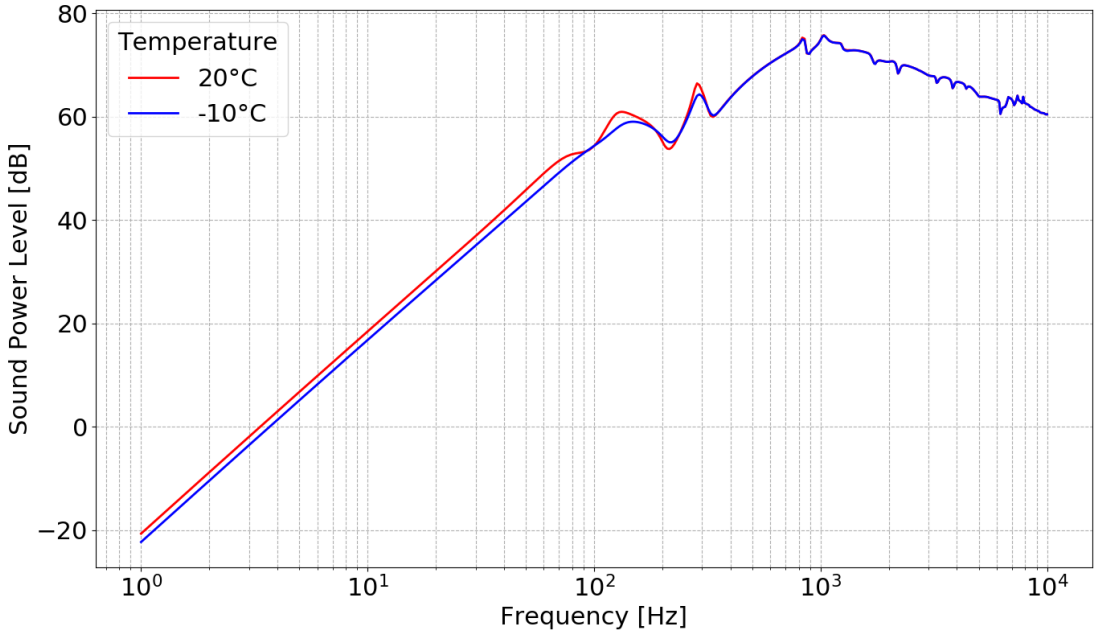

Figure 15 – Effect of the temperature on the acoustic performance of the SLB3007 USP for a vertical excitation

5 Pass-By situation

To conclude this report, the influence of the USP over a pass-by events is given in Figure 16. As expected the effect of the USP is present only in the low frequency range. At the maximum, the pressure level for track with USP installed is 1dB above the pressure level of the reference track.

This pass-by calculation take into account the components of noise from the sleepers, rail and wheels. Because of that summation, the USP effect is less important than when looking at the track alone as presented in the previous sections.

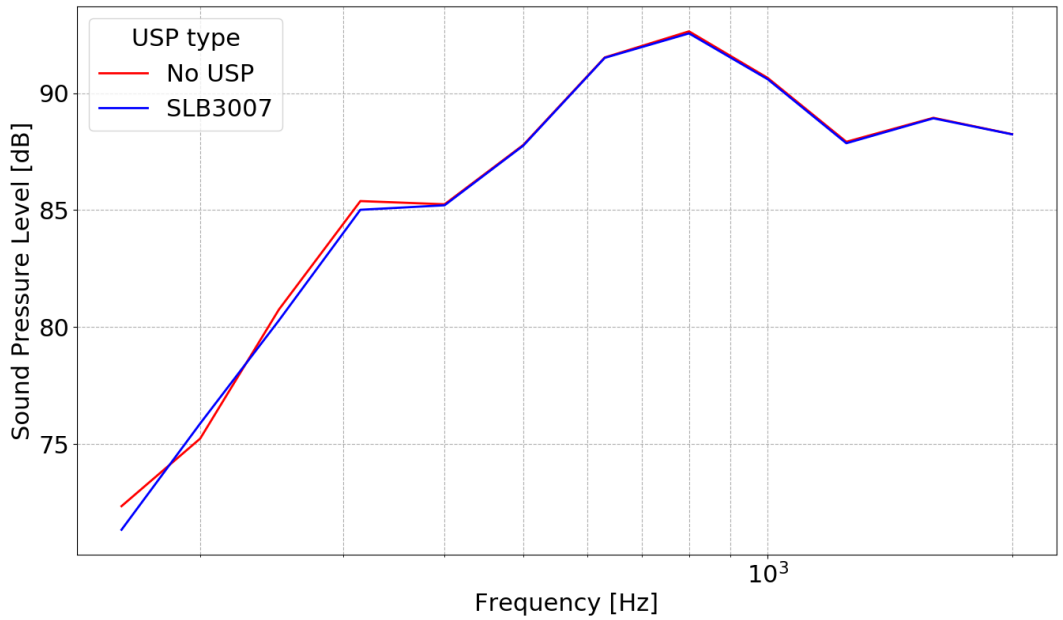

Figure 16 – Sound Pressure Levels for a pass-by event on tracks with or without hard USP installed

Conclusions

Observations and Guidelines:

- USP are soft track component with a frequency-temperature dependent behaviour. Their material properties should be measured via DMA to ensure a proper modelling of the pad properties.
- The influence of USPs over the track dynamics and acoustic is limited to frequencies up to 30 Hz for a lateral excitation and up to 300 Hz for a vertical excitation.
- Only the USP stiffness matters when looking at noise emission. The damping does not have any noticeable effect. This is due to the damping of the ballast being already very high. Any added damping is superfluous.
- At (very) low frequencies, USPs can results in a sound power level increase of around 15 dB in the lateral case and around 10 dB in the vertical case, when compared with a track without USP. These extremum are obtained for unrealistic low values of USP stiffness and serve only as guidelines.
- Since the temperature has an effect on the USP stiffness, care should be taken to measure reference track and track with USP at at comparable temperature conditions and if possible at close locations.
- For pass-by events, the presence of hard USP (SLB3007) results in a maximum increase of the Sound Pressure Levels by 1dB.

Update on project modules:

Modules	State	Comments
1		Material characterization is done
2-4		Analytical model for lateral and vertical track dynamic
5		Extension of the analytical model to acoustic
6		Model validated on Effretikon measurements
Reporting		Final report written

Labels:

Done	In progress – On time	In progress - Delay

Update on budget:

Labels	Budget [CHF]
Salary 50% Post Doc – 9 months	50750
Sleeper Measurements Expert	4300
Project Management (5%) – 9 months	3252
Total	58302
Remaining from project budget	10000

References

1) *Railway Noise and Vibration: Mechanisms, Modelling and Means of Control*. D. J. Thompson, Elsevier 2008.
2) *A model of a discretely supported railway track based on a 2.5D finite element approach*. X. Zhang et al., Journal of Sound and Vibration, 2019.
3) *Analysis of lateral vibration behaviour of railway track at high frequencies using a continuously supported multiple beam model*. T. X. Wu and D. J. Thompson, J. Acoust. Soc. Am, 106, 1999.

Appendix

1) 3 months report
2) 6 months report
3) 9 months report

Empa
Materials Science and Technology

Rail Track Noise Emission
Influence of Under Sleeper Pads on Railway Rolling Noise Emissions

Technical Report – 3 Months

Laboratory for Acoustics and Noise Control

Empa
Überlandstrasse 129
8600 Dübendorf, Switzerland

Dübendorf, 14 January 2018

Dr. Benjamin Morin

Project Reference: O315-0323
Empa Number: 5211.01578.100

Zusammenfassung

Der vorliegende Bericht fasst die erzielten Ergebnisse zusammen, welche in den ersten drei von insgesamt zwölf Monaten Projektdauer erarbeitet wurden.

Nach einer kurzen Einführung in das Thema Schwellenbesohlung werden die Eigenschaften der von den SBB verwendeten Besohlungsmaterialien präsentiert. In einem nächsten Schritt wird der Einfluss der Schwellenbesohlung auf die Track Decay Rate mit einem an der Empa entwickelten analytischen Modell untersucht. Ein bereits teilweise vorhandenes Modell, welches im Rahmen des Rail Pad Projektes entwickelt wurde, musste zuerst entsprechend erweitert werden. Das analytische Modell erlaubt schon jetzt erste Parameterstudien, in denen der Effekt der Materialeigenschaften der Besohlung auf die TDR sehr zeiteffizient untersucht werden kann. Erste Modellvalidierungen wurden bereits basierend auf aktuellen Messdaten im realen Gleis vorgenommen. Schliesslich werden im Bericht sowohl ein aktualisierter Zeitplan als auch eine Budgetübersicht dargestellt.

Die verwendeten Referenzen sind am Schluss des Berichtes aufgeführt.

Summary

This report resumes the first three months of the project *Rail Track Noise Emission - Influence of Under Sleeper Pads on Railway Rolling Noise Emissions,* as set in the project contract.

The document first gives a short introduction into USP technology and presents a review of the products currently used or selected by SBB and their important properties.

Then the influence of these USPs on the Track Decay Rate is investigated using an in-house analytical model for track dynamics and the effects of USP parameters are investigated.

In the third part, the model is compared with in-situ measurements for validation.

Finally, schedules and budget are updated and the report ends with a reference section.

Table of content

I – Module 1: Analysis of existing materials and parts

Under Sleeper Pads (USPs) have been introduced in the railway industry to limit the transfer of vibrations from the sleepers to the ballast. They offer protection against both sleeper fracture and ballast deterioration which greatly reduces the maintenance costs while preserving the infrastructure and expanding its life-time [1-6]. The effectiveness of such pads comes from the load distribution over a broader surface of ballast (see Figure 1).

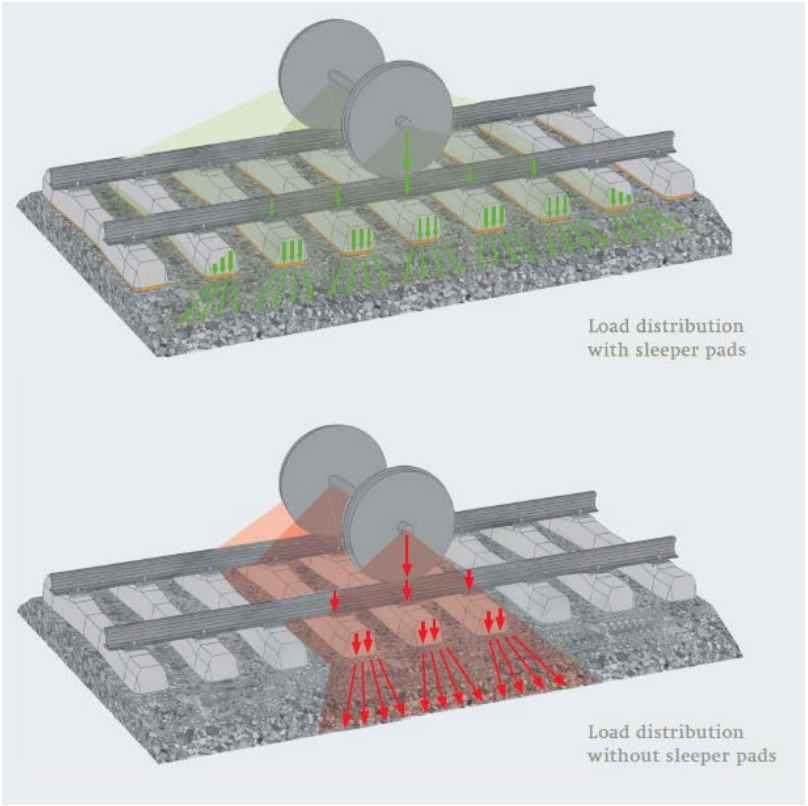

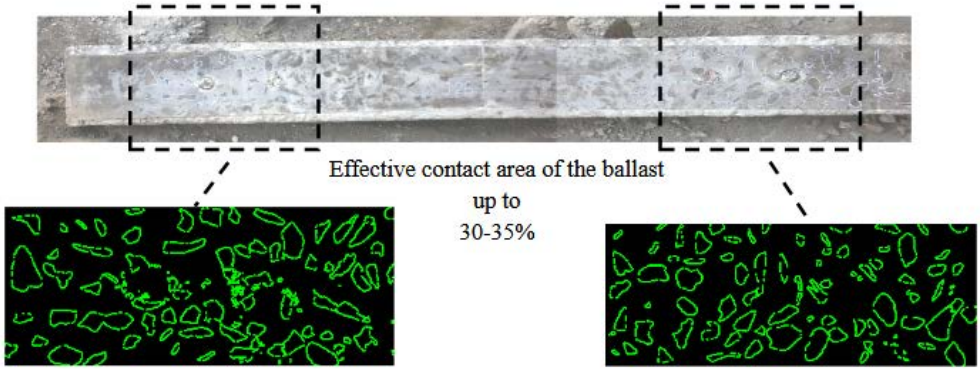

**Figure 1 – Illustration of better load distribution [7]
and digital contact area analysis conducted by Getzner [8]**

Three USPs have been selected by SBB for a possible use on the Swiss railway network. Following the SBB report [9], these pads are denominated as soft, medium and hard depending on their relative stiffness.
The pad manufacturer, Getzner, is specialized in the production of polyurethane foam solutions for building acoustic and railway super-structures. The foam formulation allows for an extensive number of stiffness and damping combinations. Three classes of foam are available from Getzner: the Sylomer [10], Sylodyn [11] and Sylodamp [12]. The main distinction between these classes comes from the share of open/close cells in the material. The Sylomer class contains open cells and offers good damping properties while the Sylodyn contains closed cells which results in a stiffer material better adapted to heavy loads and protection from chocks. The last class, Sylodamp, use a mix of both open and closed cells and is presented as the best of both worlds for stiffness and damping.
Two of the selected pads, the SLB 2210 G [13] (Medium) and SLB 3007 G [14] (Hard), are made of Sylomer while the last pad, SLN 1510 G [15] (Soft), is made of Sylodyn. Their dynamic stiffnesses (at 10Hz) are calculated based on the bedding modulus given in [13-15] and the surface of contact taken as a B91 sleeper lower face half area (3.05e5 mm^2) [9]. These dynamic stiffnesses are reported in Table 1. No loss factors are given in the pads overview reports [13-15], however from the Sylomer and Sylodyn overview reports [10] and [11] a loss factor range can be estimated for each pad. These estimated factors are also reported in Table 1.

	Dyn. Stiff. @ 10Hz (MN/m)	Estimated Loss Factor Range
SLN 1510 G (Soft)	48.8	0.07-0.1
SLB 2210 G (Medium)	134.2	0.11-0.25
SLB 3007 G (Hard)	176.9	0.11-0.25

Table 1 – Dynamic stiffness and estimated loss factors of selected pads

The dynamic stiffness and the loss factor are enough information for a first evaluation of the influence of the pads on track dynamics (see next section). It should however be noted that at the moment both parameters are considered constant which represents an over-simplification of the reality, commonly used by manufacturers and railway companies.
To better represent the physics, Dynamical Mechanical Analysis (DMA) measurement data would be needed to model and fit the frequency dependent behaviour of the pads through the dynamic stiffness and the loss factor.
At the beginning of the project these DMA data where supposed to be given by Getzner directly. However after recent talks it seems that Getzner doesn't possess such data. To solve this issue it has been decided that DMA will be conducted at Empa while Getzner will provide pad material samples. Although this represents an added workload, this will not slow down the other parts of the project as the numerical models can be extended and

used based on parameters in Table 1. When the DMA is done and the required set of parameters is obtained, a simple switch of parameters will be done in the numerical models.

II – Module 2: Extend existing models for vertical dynamics of track

The track dynamics model used in this project is an extension of the analytical model developed at Empa for the *Novel Rail Pads for improved Noise Reduction and Reduced Track Maintenance* project [16].
The aim of this previous model was to provide a rapid assessment of the effects of new rail pad geometries and materials on track dynamics and acoustics to complement the more detailed Finite Element Modelling (FEM) studies. The model is based on the analytical representation of tracks found in [17] and one of its novelties is to account for the frequency dependence of the rail pads dynamic stiffness and loss factor. These parameters are then used to calculate the total complex stiffness at each support bay (see Figure 2).

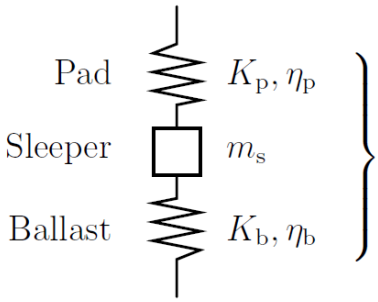

$$K(\omega) = \frac{K_p(1+\mathrm{i}\eta_p)\left(K_b(1+\mathrm{i}\eta_b) - \omega^2 m_s\right)}{K_p(1+\mathrm{i}\eta_p) + K_b(1+\mathrm{i}\eta_b) - \omega^2 m_s}$$

Figure 2 – Frequency dependent complex support stiffness

Another improvement from this model is to account for the rail bending in the vertical plane in addition to the vertical deflection from the state of art model. From the rail displacements the Track Decay Rate (TDR) can then be derived following the standard EN 15461 [18].
To account for the influence of the USPs on the track response, the stiffness layer previously accounting for the ballast have been replaced with an equivalent stiffness representing both USP and ballast as two complex springs connected in series. The parameter *Kb* is thus replaced by an equivalent stiffness *Ke = 1/(1/Kb + 1/Ku)* where *Ku* is the USP complex stiffness.
This extended model has been applied to the three sets of parameters from Table 1 and the influence of the USPs on the vertical TDR is shown in Figure 3. The model predicts a drop of the TDR amplitudes before the first resonance, about an order of magnitude at most. This is due to the fact that the USPs stiffnesses have lower values than the ballast

stiffness. In the presence of USPs the lower layer of springs is then softer and this changes the track response by allowing more rail motion and vibrations.
The results also show almost no differences between medium and hard USPs while the soft one results in a more severe TDR drop.

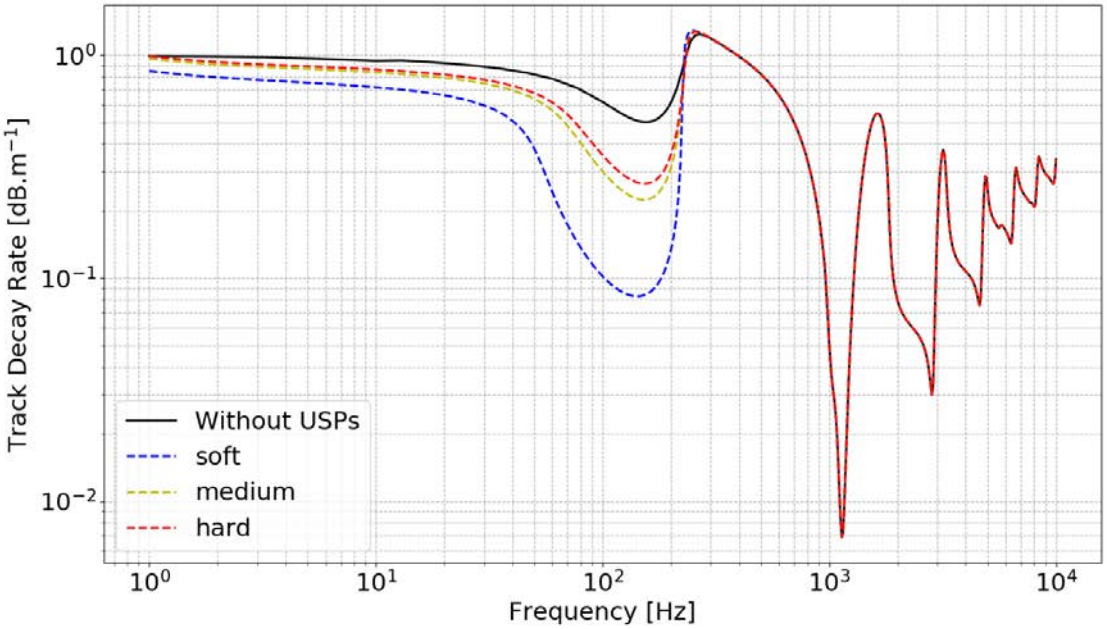

Figure 3 – Influence of existing USPs over the TDR

At this point it seems that USPs, independent of the type chosen, should be avoided when noise emission reduction is the goal. As the TDR gets really low the vibration of the rails is assured to increase which will results in more noise emitted. There are however a few factors to account for:

1) The current model does not give any information about sleeper dynamics while the USPs probably have a great influence over it. Since the sleepers participate to the total noise emission, the gain of noise reduction from the sleepers should be compared to the gain of noise emission from the rails for a complete assessment of the USPs influence over the total noise emission.
2) At the moment the model lacks the ability to predict any lateral dynamics. Since lateral TDR also affects the total noise emission levels, the influence of USPs cannot be considered fully investigated until lateral motion is included to the model.
3) The USPs tested here are all already existing on the market. Their properties are designed by manufacturers to achieve optimal track maintenance, not reduced noise emissions. Different pad parameters could lead to better TDR and a map of the parameters influence could be drawn using the current model.

Following these remarks, the conclusions from the current report do not represent an end point for the project, as the vertical vibration of the rails are just a part of the noise sources. As scheduled in the proposal [19] point 1 and 2 will be addressed during the next 3 months of the project. Point 3 is addressed now as the current version of the model allows for such parametric study.

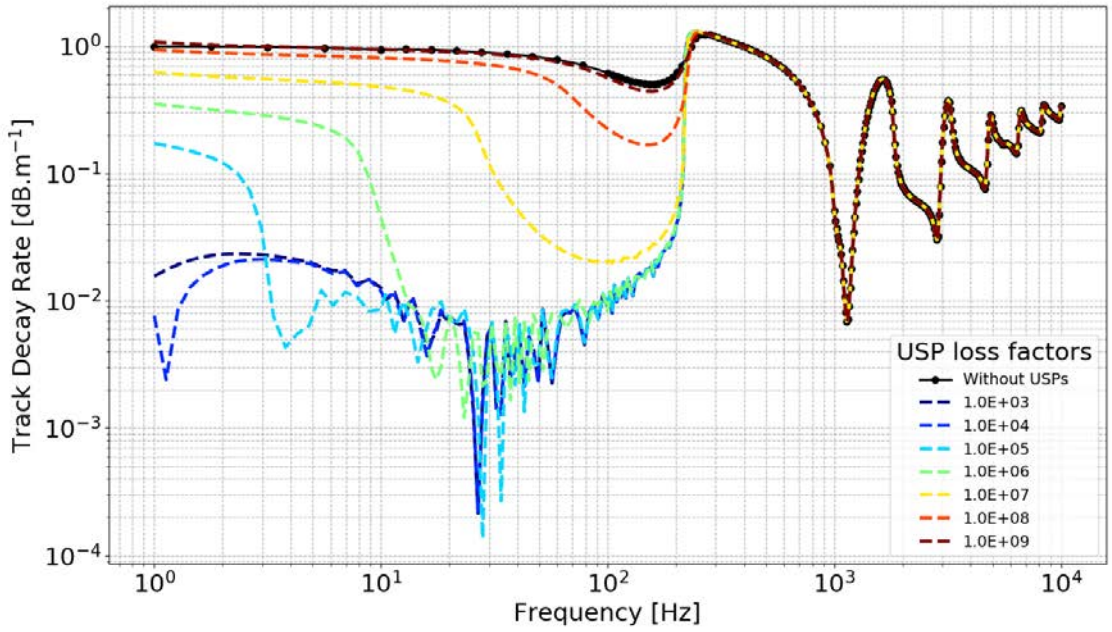

Figure 4 – Influence of USP stiffness over TDR

To start with the stiffness of the USPs is investigated and a map of TDRs per stiffness is given in Figure 4. These results show that two plateau exists:

- When the USP stiffness reaches 1e9 N/m the pad is so stiff (even more than the ballast) that it no longer absorbs or damps vibrations. The response of the track is then the same as the case without USPs and any higher pad stiffness would results in the same TDR values.
- A lower plateau is found when the pad stiffness is of the order of 1e3 to 1e4 N/m.

As a rule of thumb, higher USP stiffness correlates to better TDR amplitudes. It is then tempting to assume that the problematic of the project could be solved with very stiff USPs, but one should not forget that the main goal of USP is track protection and better maintenance. The stiffer the pads the less they would be able to assume this protective role.

A second map is drawn in Figure 5 to show the influence of pads loss factors over the TDR.

A USP stiffness of 1e3 N/m is used here to investigate the effects of pads with similar stiffness as already existing but more dissipative. This low stiffness value would allow more track motion and thus greater TDR variations depending on the loss factor, thus helping to show its influence. The result is however disappointing as almost no difference is found between the low damping pad and even unrealistically high damping one.

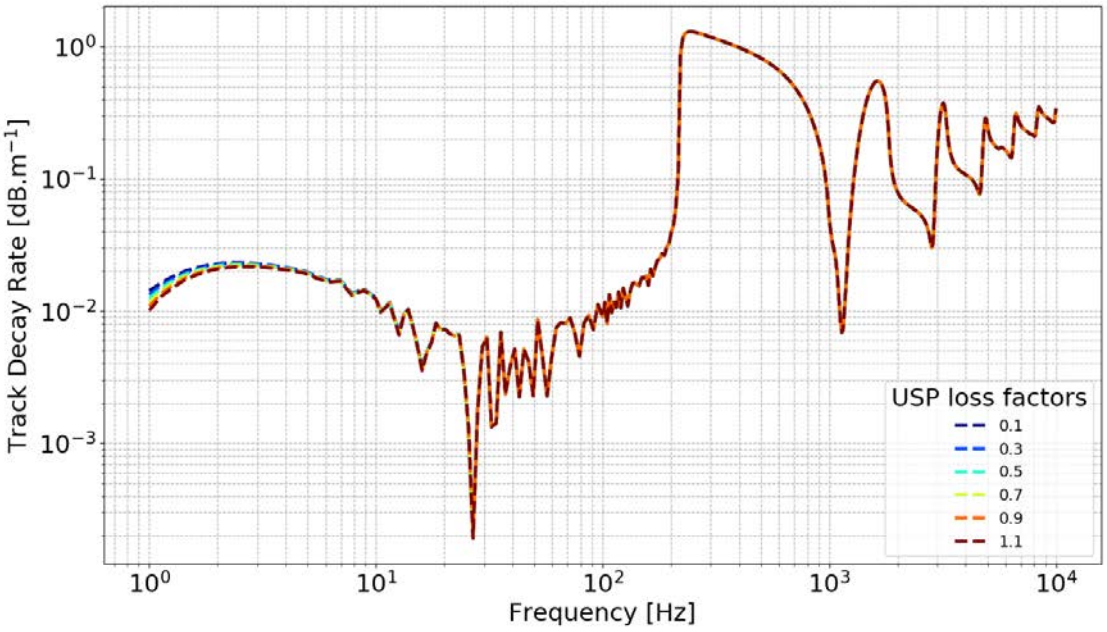

Figure 5 – Influence of USP loss factors over TDR

The analytical model developed previously at Empa has been extended to account for presence of USPs in the track super-structure. The pads are represented by their vertical stiffness and loss factors. The bending stiffness and loss factor can be added to the current version of the model similarly to what is done for the rail pads. However, these parameters are not given by the manufacturer and DMA would be required first to calculate them. As stated in the first section, such measurements are delayed. When the DMA is done then the vertical bending will be added to the model.

From the extended model it was shown that current USPs solutions are predicted to result in a drastic drop of the TDR in the low frequency range, resulting in an increase of the noise emissions. It has to be noted that this concerns only the vertical TDR. USP may or may not increase lateral TDR and may or may not decrease sleeper vibrations. Both quantities are at the moment missing from the model and will be added following the schedule from the proposal [19]. The conclusions from this report should thus be considered as exploratory rather than a dead end.

The difference between the three selected pads is almost none, indicating that there may be way for improvements via the pads parameters. Following this idea two maps of TDR

responses have been calculated to investigate the effects of USP stiffness and loss factor over the track dynamics. The results can be summarized as:

- Stiffer pads would lead to better TDR at the cost that the protective role of USP may no longer be achievable.
- Loss factor doesn't affect the TDR.

III – Module 6: Compare numerical results with experimental data

In October 2018, a set of in-situ measurements have been conducted by Empa on a segment of track between Effretikon and Winterthur. The track components for this segment are given in Table 2 (Verified with SBB).

Rails	UIC 60E2
Sleepers	B91
Rail Pads	Zw 661a
Clamping	W14
Under Sleeper Pads	SLB 3007 G

Table 2 – Measured track components

The vertical TDR of this segment has been measured (see Figure [5]) following the standard [18] and is used here for the validation of the analytical model.

Figure 5 – TDR measurements at Effretikon site

The comparison between measurements and simulation is shown on Figure 6, where 3 types of loading are considered with the model: excitation on sleeper, at quarter span and mid span.

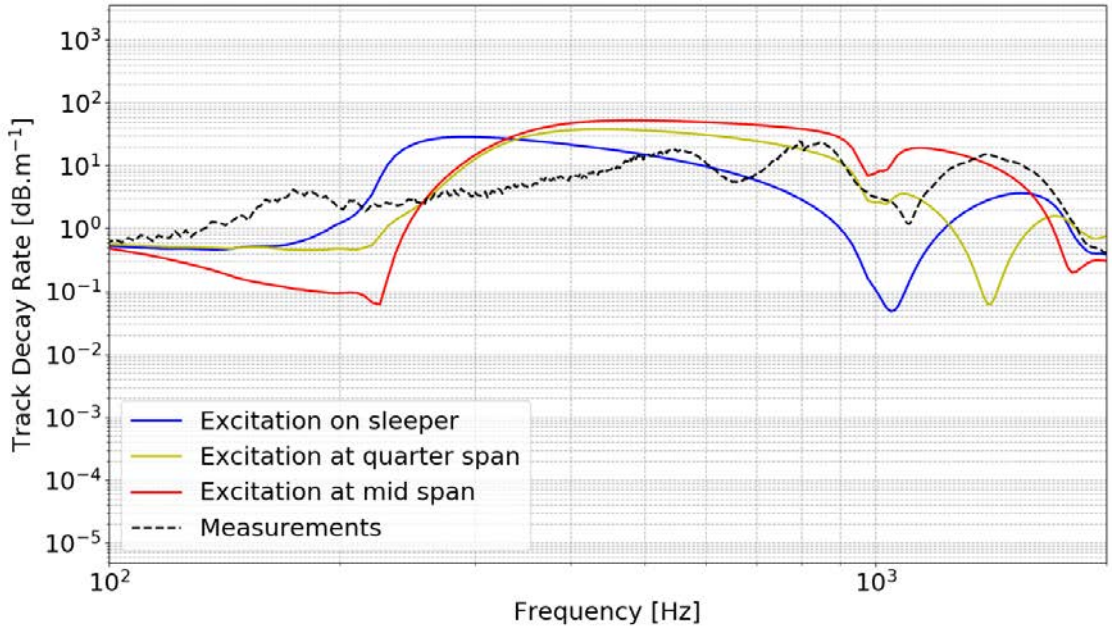

Figure 6 – Comparison of the analytical model with measured TDR

A first observation is that the measured TDR amplitude and the calculated TDRs amplitudes fit very well in terms of order of magnitude.
The cut off frequency of the measurements (first resonance around 550 Hz) is approached by the model without totally fitting it: This frequency depends on the rail pads stiffness and in the current simulation this value is chosen after trial and errors since the clamping system preload and the ageing of the rail pads are not modelled. The result is however in good accordance with the experiments.
At high frequency the TDR amplitudes still match and the last peak of the measured response seems to be captured by the analytical model. The two previous peaks of the measured curve are not well represented by the model. This can be explained by the lack of ground representation in the model where the ballast is the last layer. Since the model contains only two layers of springs, only two peaks are simulated. Adding a ground stiffness and a ballast mass to the model would result in the presence of a third resonance in the simulation but would not add any other improvements.
Also the bending stiffness of the USP is not represented (DMA required) in the current model which may lead to some of the differences observed here between simulations and measurements.

Conclusions: The initial setup has been proven to be valid but the models need to be further developed according to the steps defined in the project proposal [19].

IV – Timing and Budget

Labels:

Done	In progress – On time	In progress - Late

Update on project modules, at the 10th January 2019:

Modules	State	Comments
1		DMA not available from Getzner, simple delay
2		-
3		
4		
5		
6		-
Reporting		3 months report written, next one for 6 months

Update on project budget, at the 10th January 2019:

Labels	Budget [CHF]
Salary 50% Post Doc – 3 months	12687.50
Project Management (5%) – 3 months	813.00
Total	13500.50
Remaining from project budget	54801.50

V - References

1. *Analysis of the Performance of Under Sleeper Pads - A Critical Review*. C. Jayasuriya, B. Indraratna, S. Nimbalkar. ICGE Colombo, 2015.
2. *The effects of under-sleeper pads on sleeper-ballast interaction.* P. J. Gräbe, B. F. Mtshotana, M. M. Sebati, E. Q. Thünemann. J. S. Afr. Inst. Civ. Eng., Vol 58, Num 2, 2016.

3. *Mitigation of Ground Vibration Generated by High-Speed Trains on Saturated Poroelastic Ground with Under-Sleeper Pads*. Z. Cao, Y. Cai, and J. Han. Journal of Transportation Engineering, Vol 141, Issue 1, 2015.
4. *Experimental investigation of railway track with under sleeper pad*. S. Lakušić, M. Ahac, I. Haladin. 10th Slovenian road and transportation congress (pp. 386–393). Ljubljana, 2010.
5. *Rail traffic noise and vibration mitigation measures in urban areas*. S. Lakušić, M. Ahac. Technical Gazette, 19, 427–435.
6. *Measurement report about a new under sleeper test track in a curve*, Deliverable D3.8. Railway Induced Vibration Abatement Solutions, 2013.
7. *Sleeper pads for ballasted track*. Getzner Werkstoffe GmbH.
8. *Reduction of Vibration Emissions and Secondary Airborne Noise with Under-Sleeper Pads –Effectiveness and Experiences*. H. Loy, A. Augustin, L. Tschann. Getzner Werkstoffe GmbH.
9. *Technische Spezifikation Schwellenbesohlung*. SBB AG, 27 April 2014.
10. *Data Sheet Overview Sylomer*. Getzner Werkstoffe GmbH.
11. *Data Sheet Overview Sylodyn*. Getzner Werkstoffe GmbH.
12. *Data Sheet Overview Sylodamp*. Getzner Werkstoffe GmbH.
13. *Sylomer Schwellenbesohlung SLB 2210 G*. Getzner Werkstoffe GmbH.
14. *Sylomer Schwellenbesohlung SLB 3007 G*. Getzner Werkstoffe GmbH.
15. *Sylomer Schwellenbesohlung SLN 1510 G*. Getzner Werkstoffe GmbH.
16. *Novel Rail Pads for Improved Noise Reduction and Reduced Track Maintenance, Intermediate Report 2*. H. Frauenrath, 2018, EPFL.
17. *Railway Noise and Vibration: Mechanisms, Modelling and Means of Control*. D. J. Thompson, Elsevier 2008.
18. *Railway applications - Noise emission - Characterisation of the dynamic properties of track sections for pass by noise measurements*. EN 15461, 2006, European committee for standardization.
19. *Railway Track Noise Emission – Influence of Under Sleeper Pads on Railway Rolling Noise Emissions, Project Proposal.* B. Morin, 2018, Empa.

Empa
Materials Science and Technology

Rail Track Noise Emission
Influence of Under Sleeper Pads on Railway Rolling Noise Emissions

Technical Report – 6 Months

Laboratory for Acoustics and Noise Control

Empa
Überlandstrasse 129
8600 Dübendorf, Switzerland

Dübendorf, 5 April 2019

Dr. Benjamin Morin

Project Reference: O315-0323
Empa Number: 5211.01578.100

Zusammenfassung

Der vorliegende Bericht fasst die erzielten Ergebnisse zusammen, welche in den zweiten drei von insgesamt zwölf Monaten Projektdauer erarbeitet wurden.
Im vorliegenden Bericht wird zuerst eine leichte Umstrukturierung der ursprünglich definierten Module erklärt und begründet. In einem zweiten Teil wird auf die von GETZNER zur Verfügung gestellten Materialdaten eingegangen. In einem dritten Teil werden Resultate von Messungen an besohlten Schwellen und die Validierung des entsprechend erweiterten dynamischen Oberbaumodells diskutiert. Und in einem letzten Abschnitt wird auf die Berechnung des abgestrahlten Luftschalls und den Einfluss der Besohlung auf ebendiesen eingegangen.
Schliesslich werden im Bericht sowohl ein aktualisierter Zeitplan als auch eine Budgetübersicht dargestellt.
Die verwendeten Referenzen sind am Schluss des Berichtes aufgeführt.

Summary

This report resumes the second period (months 4-6) of the project *Rail Track Noise Emission - Influence of Under Sleeper Pads on Railway Rolling Noise Emissions,* as set in the project contract.
The document first explains the re-planning of the modules from the proposal and the reasons why such a change is required and for the best. In a second part the pads material properties of the pads are discussed since material data have finally been received from GETZNER. The third part presents the measurement of sleepers with USP and the validation of a full length sleeper model and the fourth part presents how this model is used to extend the track dynamic model already available. The last part is about noise emission estimation and the influence of USPs on it.
Finally, schedules and budget are updated and the report ends with a reference section.

Table of content

I – Modules re-planning

The re-planning concerns modules 3 and 4 of the project proposal [1]. Module 3 was about the extension of the current track dynamic model to include the lateral behaviour of the track plus the full length of the sleepers instead of a simple mass/spring representation (see Figure 1).

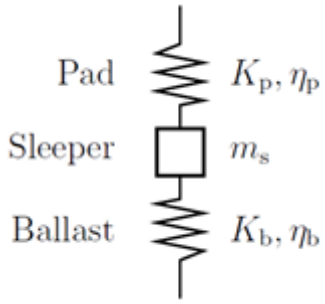

Figure 1 – Mass/Spring state of art representation of sleepers in a track

Module 4 was about the extension of the current track model to include torsional behavior of the rail to get a final model with vertical, lateral and torsional behavior included.

After a deeper look at the literature, and after working on the full sleeper modelling, it appears that a few modifications should be made on modules 3 and 4. It is however important to note that these modifications will only change the schedule of the different tasks, not the final result of the project. The modifications are listed below:

Changes for module 3:

- Module 3 will be focused on the sleeper full length modelling and how to connect it to the already existing track dynamic model as this represent already a major challenge.
- The sleeper model chosen can be found in [2] and [6] and will be validated via comparison with experiments (module 6)
- The connection of the sleeper model to the track model represents a challenge as no trace of it is found in the literature. It would allow the complete sleeper dynamic to be added to the full model instead of a single resonance frequency from the mass/spring approach.
- In order to properly develop such novelty, it has been decided that the lateral extension of the full model will be removed from module 3 to be added in module 4 instead.

Changes for module 4:

- Module 4 will be focused on the modelling of the lateral behavior of the track instead of just the torsional behavior.
- This idea originates from [2] and [7]. In these two references, the lateral behavior is shown to be a combination of bending and torsion. It is also shown that both can be modelled accurately in the desired frequency range with a unique model.
- The distinction of lateral bending and torsion in two different modules appears to be counter-productive as both are part of the same global lateral behavior of the track.
- Module 4 will thus be focused on both bending and torsion, and this fit with the modification of module 3 where the lateral bending was excluded and had to be transferred in another module in order to keep the finality of the project the same.

In the end these changes don't change the final deliverables of the project [1]. They allow a better allocation of time to tackle new challenges (connection of sleeper model to track mode) while keeping related topics together (lateral bending and torsion should be together, not in separated modules).

II – Material data from GETZNER and application (Module 1)

In the first 3 months report [1], the need for DMA (Dynamical Mechanical Analysis) in order to correctly model the frequency and temperature dependent of the USPs materials was stated. Material samples from GETZNER have been received in order to do a set of DMA characterization at Empa. These in-house measures are scheduled and will be done in the next project phases.
Meanwhile, a finite element of a half USP has been developed (see Figure 2), so that the basis for the Super-Element (SE) approach (from the rail pad project) is ready. The SE approach allows the computation of the USP stiffness at the component level, based on frequency /temperature dependant material properties and the geometry.
After a talk with GETZNER, they accepted to share their own DMA results in order to give us a larger database to work with and possibly compare results. This data concern five materials from the Sylodyn class and thus does not correspond exactly to the material used in the USPs selected by SBB. They can however be used to test the SE approach on USPs and validate it. This way no time is lost and the Empa DMA can be plugged directly into the model when ready.

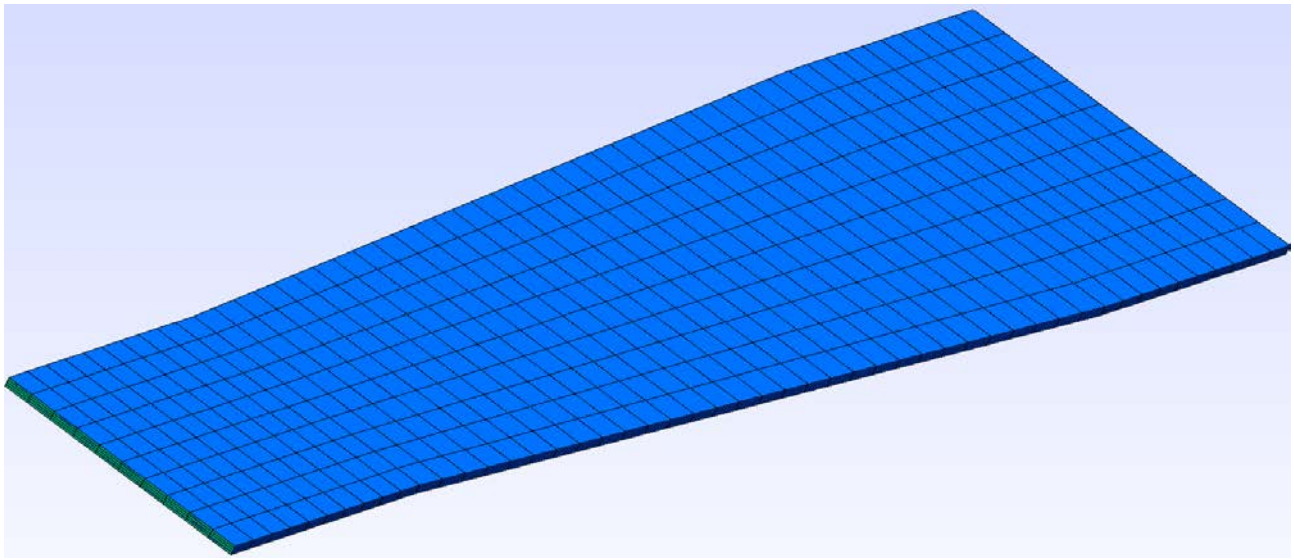

Figure 2 – Half Under Sleeper Pad finite element mesh

The storage modulus and loss factor for these five materials are shown in Figures 3 and 4 while the expected values from GETZNER documentation are stored in the table from Figure 5, for two of the five materials: HRB-3000 and HRB-6000.

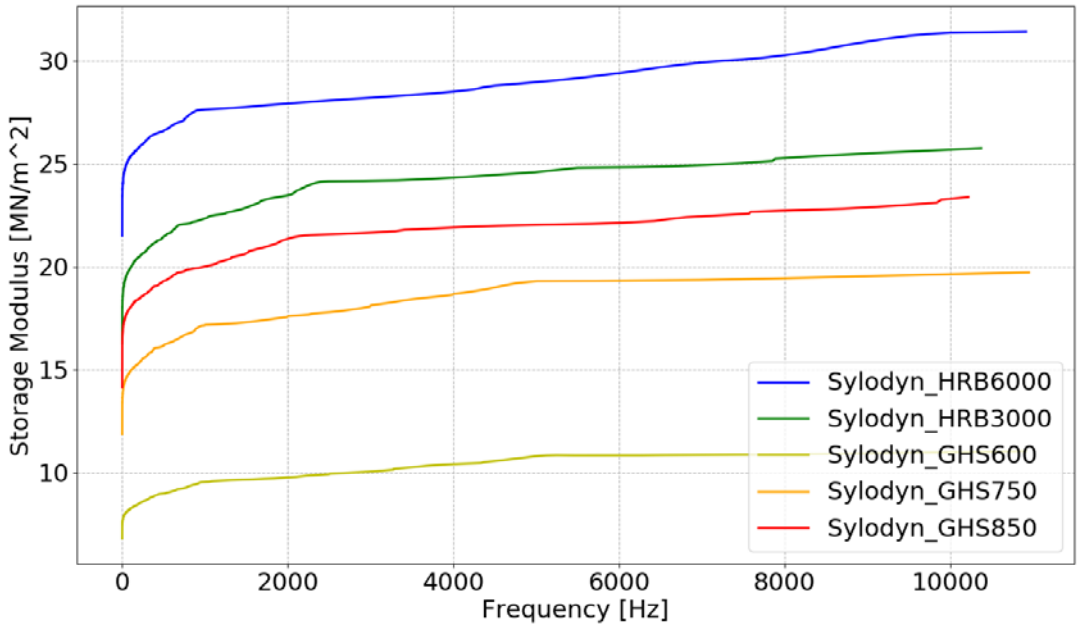

Figure 3 – Storage modulus from the GETZNER DMA data

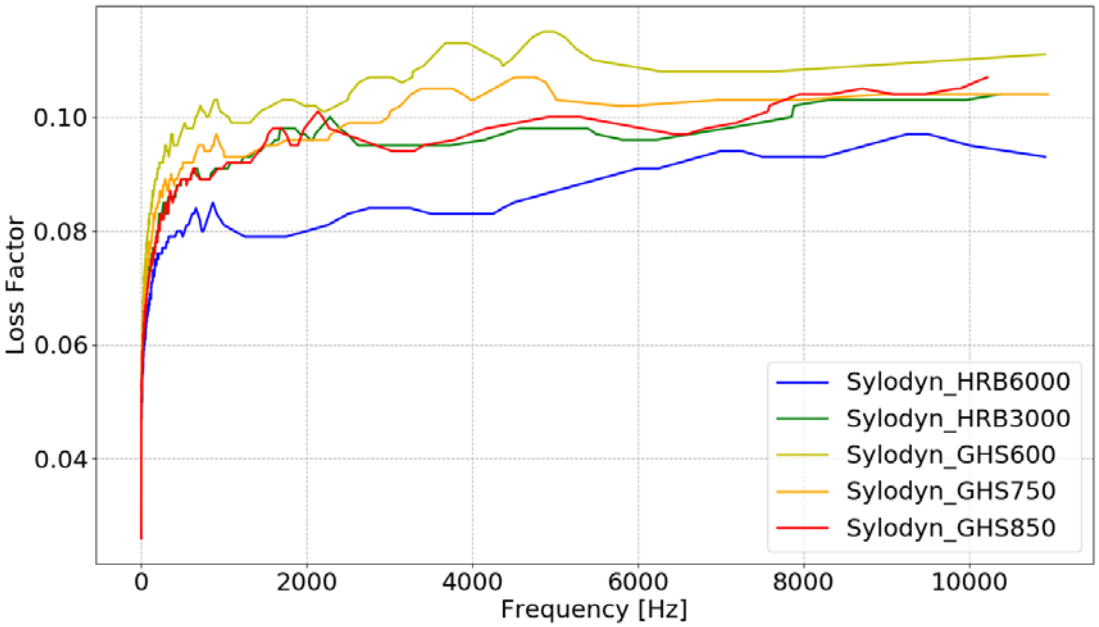

Figure 4 – Storage modulus from the GETZNER DMA data

Sylodyn® Material type

HRB HS 3000 | HRB HS 6000

Properties	Test procedures		
Color		dark green	dark blue
Static range of use[1] in N/mm²		3.000	6.000
Load peaks[1] in N/mm²		12.00	18.00
Mechanical loss factor	DIN 53513[2]	0.07	0.07
Rebound elasticity in %	EN ISO 8307	70	70
Compression set[3] in %	EN ISO 1856	< 5	< 5
Static modulus of elasticity[1] in N/mm²		33.20	74.00
Dynamic modulus of elasticity[1] in N/mm²	DIN 53513[2]	49.10	113.80

Figure 5 – Getzner material overview for Sylodyn HRB3000 and HRB6000

At first, looking at the storage modulus (Figure 3), it appears that the measured values are way under the announced values from the documentation:

- For the HRB 3000, the storage modulus (modulus of elasticity in Figure 5), should start at 33.2 MN/m^2 at 0Hz and go up to 49.1 MN/m^2 at high frequency. From the measurements, the modulus start at 17.5 MN/m^2 and end up around 25.5 MN/m^2.
- For the HRB 6000, the storage modulus (modulus of elasticity in Figure 5), should start at 74 MN/m^2 at 0Hz and go up to 113.8 MN/m^2 at high frequency. From the measurements, the modulus start at 21 MN/m^2 and end up around 31 MN/m^2.

Then, looking at the loss factor (Figure 4), the documentation gives a value of 0.07 (estimated during a low frequency measure), while the DMA also gives a value around 0.07 (around 10Hz on Figure 4). The loss factor is only a measure of the damping properties of the material (ratio between loss and storage modulus), and both documentation and DMA give the same value, which means two things:

- The frequency dependent behaviour or visco-elasticity, responsible for the damping, is well captured.
- As the loss factor is the ratio between loss modulus and storage modulus, any differences observed between documentation and DMA for the storage modulus also exist for the loss modulus, so that the ratio remain equal. This may be the result of a pre-load applied in the measurements for the documentation (as the component will be used under pre-load in the track, it make sense to gives material data corresponding to this situation in the documentation), while the DMA were performed without any pre-load (just to check the material quality after the production process).

In the end, until DMA is performed at Empa, the documentation will be used to choose the pads properties for the different models and the DMA from GETZNER will be used to validate the DMA at Empa when it will be performed.

The SE approach has been tested with the DMA data from GETZNER and the results are shown in Figure 6: the five materials have been applied to the half pad geometry in Figure 2 to compute the stiffness at the component level.
Since all materials have more or less the same frequency dependent behaviour (same increase in modulus when the frequency augments), the stiffer pads are related to the stiffer materials on the whole frequency range. Here the pads stiffness ranges between 2 MN/m^2 and 7 MN/m^2 while the pads stiffness from [3-5] ranges between 40 MN/m^2 and 110 MN/m^2. Since the DMA from GETZNER gave lower property values than the documentation, it seems normal than a pad stiffness estimated with these values are also lower than the ones from the documentation.

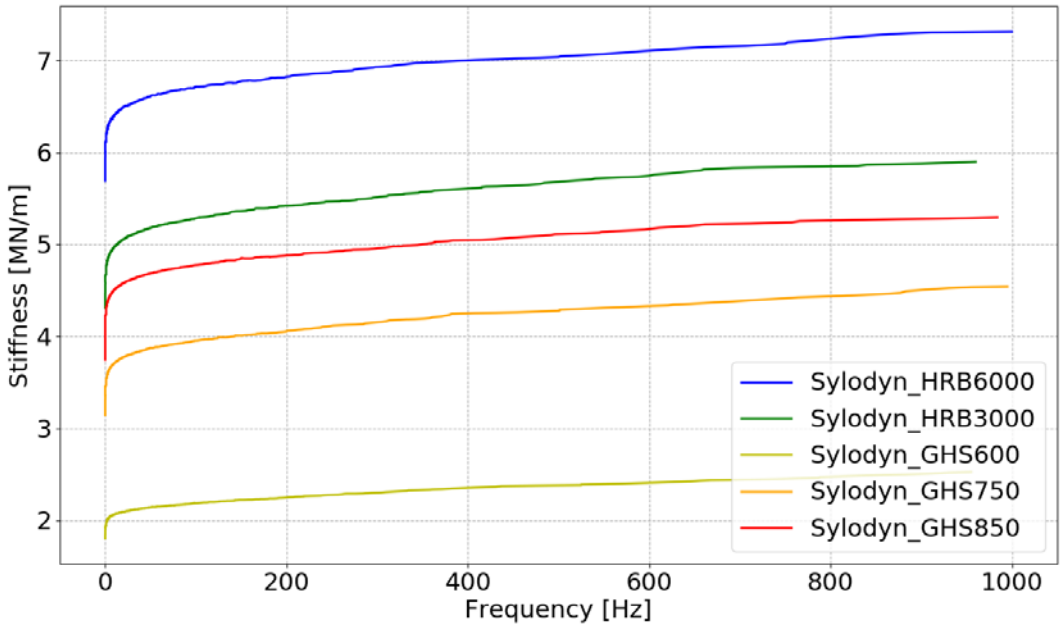

Figure 6 – USP stiffness when using the GETZNER DMA data

To conclude this part:

- Until in-house DMA is performed at Empa, the documentation from GETZNER can be used to estimate the pads parameters in the track model
- DMA from GETZNER are available for validation of the in-house DMA
- The SE approach implemented for USPs is ready so the in-house DMA data can be plugged in directly when ready

III – Sleeper modelling and validation (Module 3 and 6)

As stated in the first part, module 3 is now focused on the full length modelling of sleepers, meaning that the sleepers on ballast will no longer be accounted as a mass/spring system (Figure 1) but rather like a beam on continuous support [2, 6] where the sleeper has a length L and an harmonic excitation of amplitude F is imposed at a distance y0 from the left end (see Figure 7).

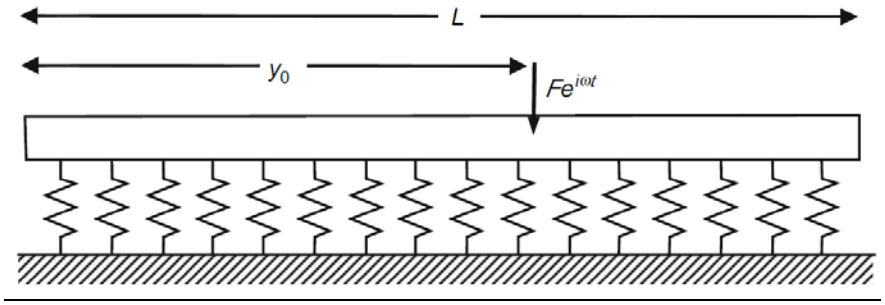

Figure 7 – Full length sleeper model

To validate this model, 3 sleepers with USPs were ordered to Vigier Rail and 2 of them have been tested at Empa. The USPs in use are of the 'hard' type specified by SBB, namely SLB 3007 from GETZNER.

Two types of tests were performed:

- Suspended: the sleepers were attached at the rail clamps and lifted a few centimeters above the ground to make sure that the lower face was free.
- Supported: the sleepers were resting on the floor, thus compressing the USPs.

In each case, at one sleeper end a sweep excitation was imposed while at the other end two accelerometers measured the sleeper vertical vibrations. For the first sleeper tested, a scanning laser Doppler vibrometer was also used to measure the deformations and get the mode shapes of each resonance. The set up for these measurements is shown in Figure 8 and 9.

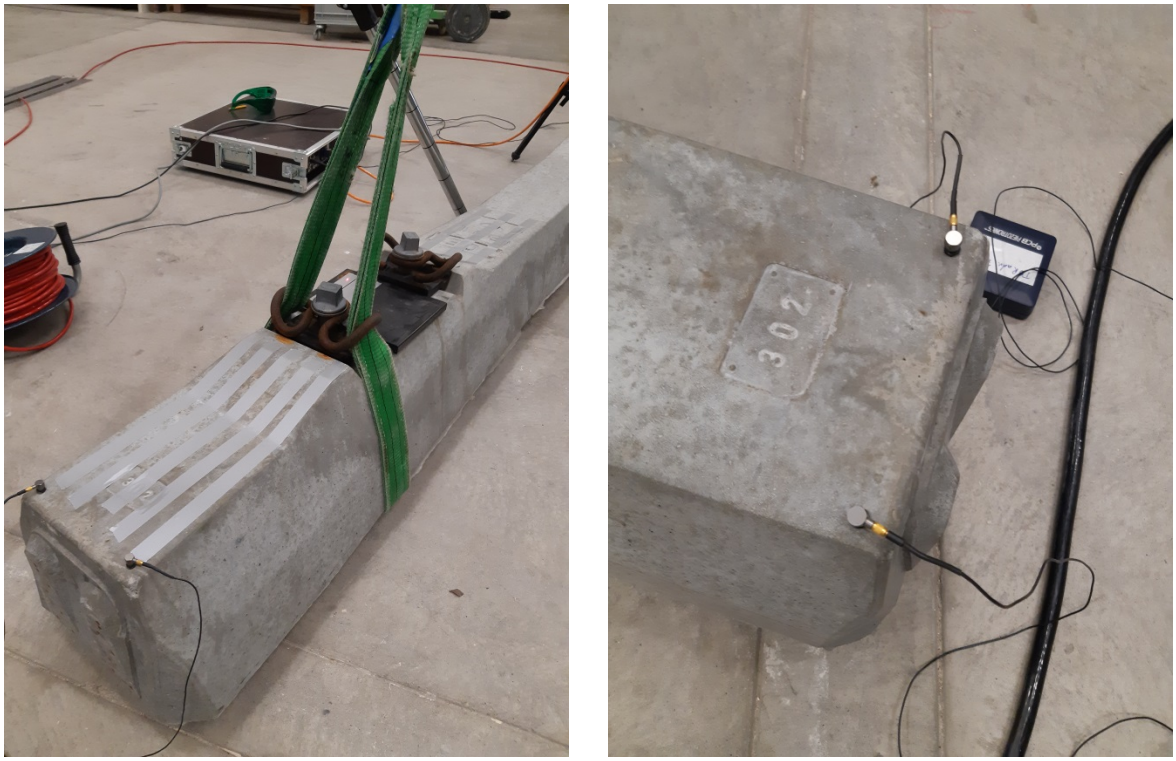

Figure 8 – Accelerometers positions, on each side to measure bending and torsion

Figure 9 – Measurements set-up

The comparison between the acceleration transfer function (accelerance) of the suspended and supported cases for the first sleeper is presented on Figure 10. It clearly shows a shift of the resonances toward higher frequencies when the sleeper is supported. This shift is stronger for the resonances in the low frequency range as expected from [2]. Above a certain frequency (here between 1500Hz and 2000Hz) the resonance frequencies of the suspended and supported beams can be considered equal, meaning that the support only affects a limited frequency range.

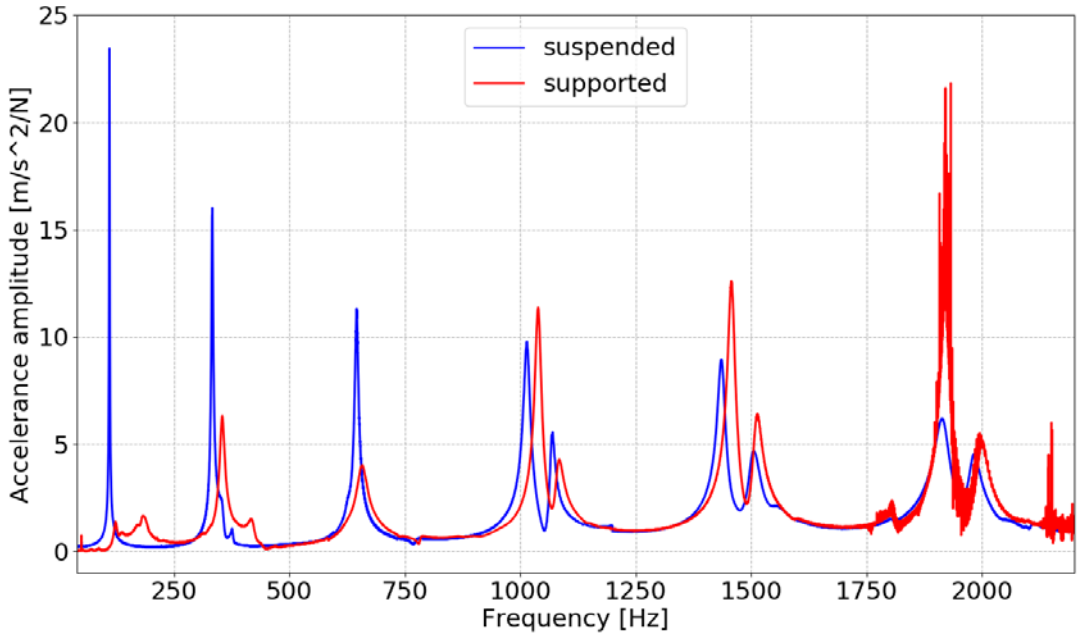

Figure 10 – Measured accelerance for both suspended and supported sleepers

The first bending mode of the suspended sleeper is clearly visible around 110Hz. For the supported sleeper, the situation is different as a few 'almost free modes' occur around the same frequency. This comes from the fact that the USPs are soft enough to allow some of the rigid body motion of the sleepers to appears, although at frequencies between 10Hz and 100Hz instead of 0Hz, and with mixed shapes. Thus, the energy that should go into the first bending modes is partially going into rigid-like modes. The first bending mode of the supported sleeper appears at 185Hz which correspond to a 40% deviation, and its amplitude is greatly reduced.
For the next five bending modes, the identification is easier and the comparison between suspended and supported modes is possible. Their shapes, captured with the scanning laser Doppler vibrometer, are given in Figure 11 with their respective frequencies of occurrence and the corresponding deviations.

It is clear from the descending values of the deviation that the high frequency resonances are identical, thus indicating that the support or boundary condition at the lower face only matter in the low to medium frequency range. This observation fit with the project report for the first 3 months where it was stated that the USPs only have an influence on the track dynamic in the low to medium frequency range.

Modes suspended	Modes supported	Deviation
 333Hz	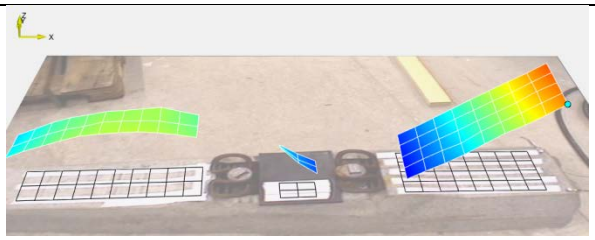 354Hz	6%
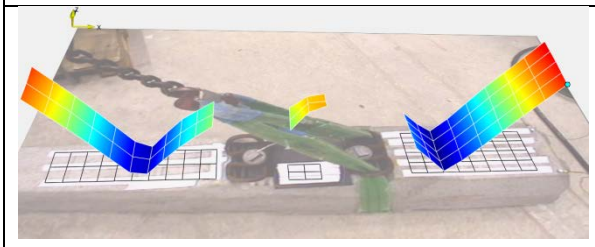 641Hz	 660Hz	2.8%
 1015Hz	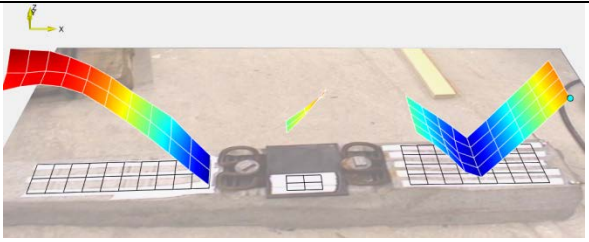 1040Hz	2.4%
 1437Hz	 1459Hz	1.5%
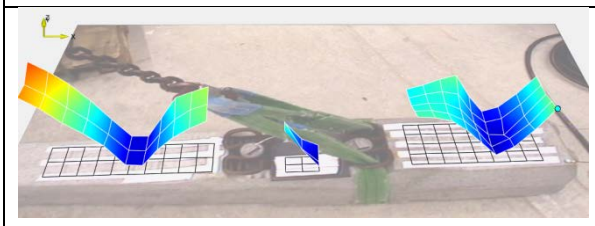 1912Hz	 1921Hz	0.4%

Figure 11 – Bending modes of the suspended and supported sleepers, with frequencies and deviation

Coming back to the sleeper model, its simulated response is shown in Figure 12 and 13, for a suspended or supported sleeper. The parameters for the sleeper (Young modulus, density, etc…) are taken from a B91 sleeper finite element model defined at EPFL by Joël Cugnoni while the parameters for the USP (stiffness and loss factor) are taken from the GETZNER USP documentation [3-5].

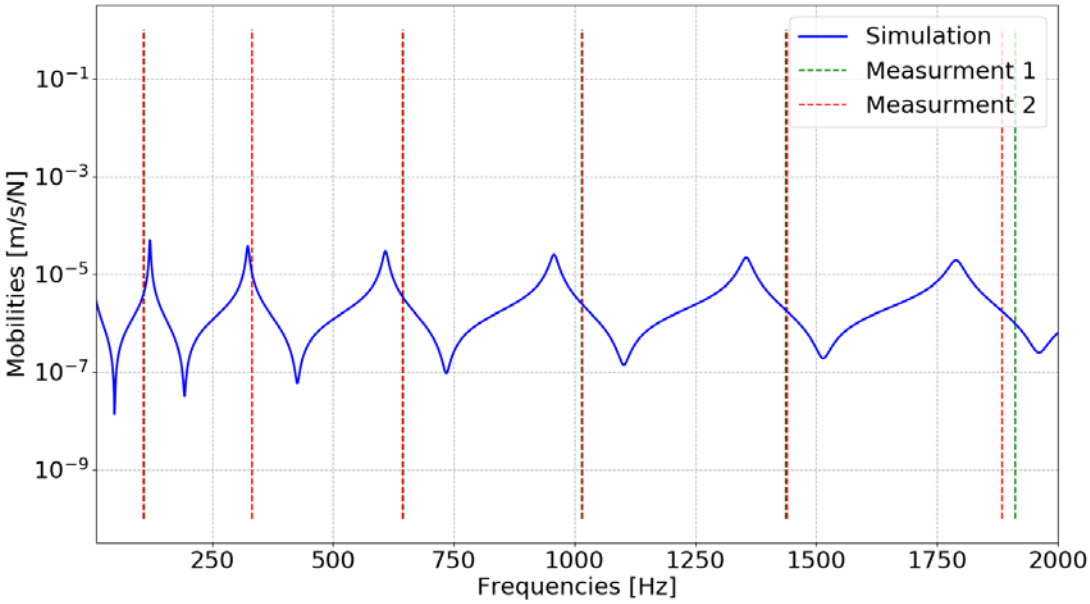

Figure 12 – Simulated mobilities in the suspended case, compared to the resonances from both measured sleepers

In both cases the resonances in the low frequency range are well captured while the resonances in the medium/high frequency range get shifted more and more. This shift is due to the way the sleeper is modelled, as a trapezoidal beam with uniform cross section along its longitudinal axis. In reality both sleeper ends are larger than the center part, which means that some mass is missing at both ends of the model.

Two features seen on Figures 12 and 13 come from this hypothesis:

- In the suspended case, the first resonance is equal to the square root of the young modulus over the density, and the missing mass can be seen as missing density. The

first resonance of the model is thus occurring at slightly higher frequency compared to the measurements.

- Overall, this missing mass makes it easier to trigger the modes. This means a lower value of the model resonance frequencies, or a resonance shift. The value of this shift depends on how much easier it is to excite a given mode when the mass is missing. As the mass is mostly missing at the sleeper ends, any mode with a concentration of the deformation in the sleeper ends will be subject to a larger shift. Looking at Figure 11, the higher the frequency of a mode, the more deformation there is at the sleeper ends. This explains why the modes that occur at higher frequencies get shifted more and more with the model.

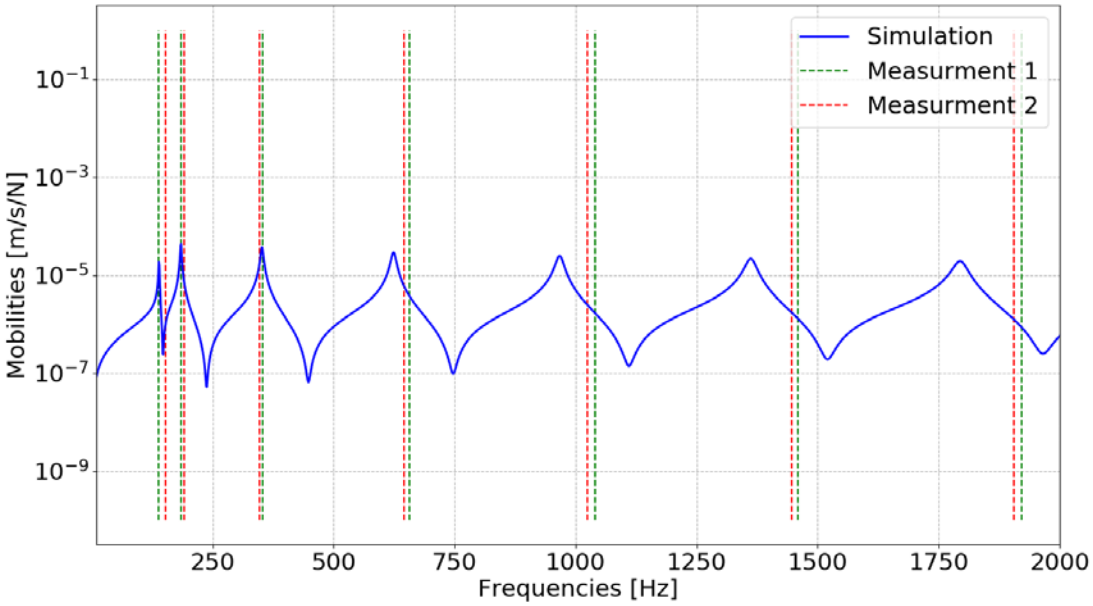

Figure 13 – Simulated mobilities in the suspported case, compared to the resonances from both measured sleepers

For the moment this represents a minor issue as the reason for these shifts is known so the current model is considered validated and won't be developed further. Later, if this sleeper resonance shifts appears to be an issue, the model can be improved to account for the larger cross sections at each sleeper ends.

IV – Connection of the sleeper model to the track model (Module 3)

A sleeper model has been defined in the previous section to replace the state of art mass/spring sleeper/ballast representation. While such model can be found in the literature, its connection to a track model has never been done so far as it was mainly used as a tool to understand the behaviour of sleepers, not full track super-structure.
The technique employed here to make the connection rely on the use of transfer functions from the sleeper model and the superposition approach of the current track model, in which each track support (rail pad, sleeper, ballast) is normally represented by an assembly of springs and mass (see Figure 1) with an equivalent dynamic stiffness.
Now, the transfer function of the supported sleeper (on USP and ballast) at the rail seat is now calculated thanks to the sleeper model and used in the place of the previous support dynamic stiffness. Only the rail pads are kept the same.
The response of the extended model is compared to the response of the original track model in Figure 14, in the case where no USPs are used so only the influence of the sleeper model over the mass/spring representation is visible, without any side effects from USP.

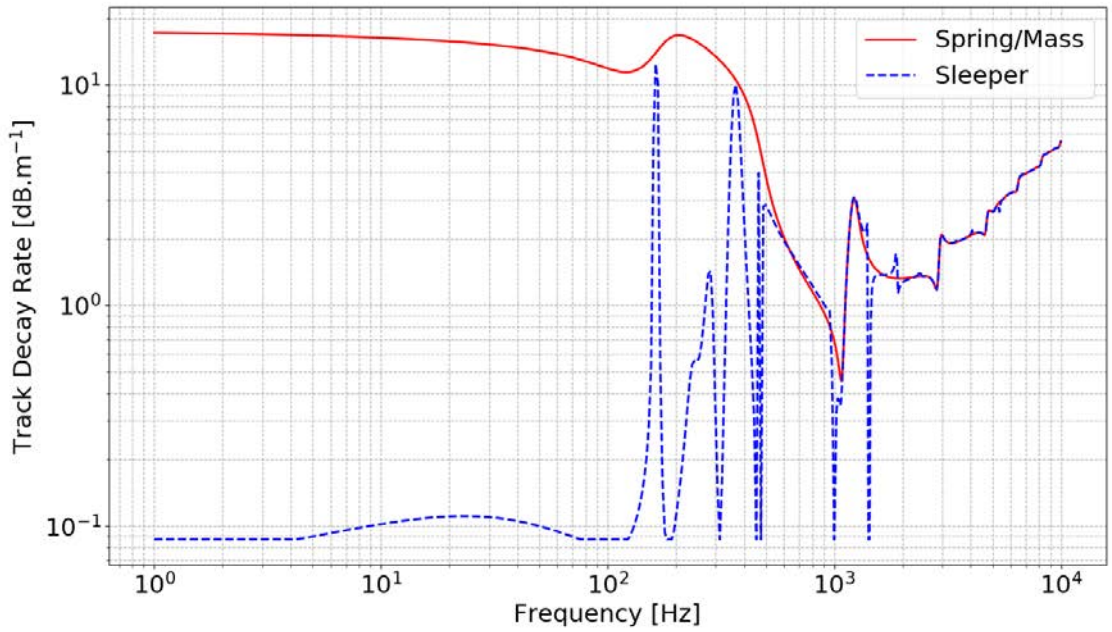

Figure 14 – Comparison between track models with spring/mass sleeper/ballast representation and supported sleeper representation

Once the cut off frequency around 300Hz-400Hz is passed, the track response depend mostly on the rail and rail pads and both models are very similar which indicate that the connection between the sleeper model and the track model is done correctly. The intro-

duction of the sleeper model is supposed to affect the low frequency response, not the response after cut off and this statement is respected.
In the low frequency range the differences are however very clear: the TDR levels start with two decades of difference and many oscillations are visible for the model with added supported sleepers.
The drop in levels is likely due to the fact that for a beam supported by a set of evenly spaced mass/springs supports (like our standard track model) band gaps are present in the low frequency range. These gaps are frequency regions where no wave propagation is possible in the beam. This is due to the support type, namely the mass and springs, not the beam itself. Since TDR are higher when wave propagation is limited, the presence of band gaps at low frequency results in higher TDR for the standard model. When the sleeper is modelled in its full length with the ballast under it the band gaps disappear and the TDR level decrease.
The oscillations that come with the new track model are linked to the resonances of the sleepers themselves. The current resonance frequencies are shifted compared to the ones measured in the previous section due to the presence of ballast: instead of having USPs alone under the sleepers, the simulation here uses ballast thus resulting in a different support stiffness.
In the previous report (for the first 3 months), it was already stated that the use of USPs was likely to result in a drop of the TDR before cut off frequency. This is already clearly visible with the standard model using mass and springs as seen in Figure 15.

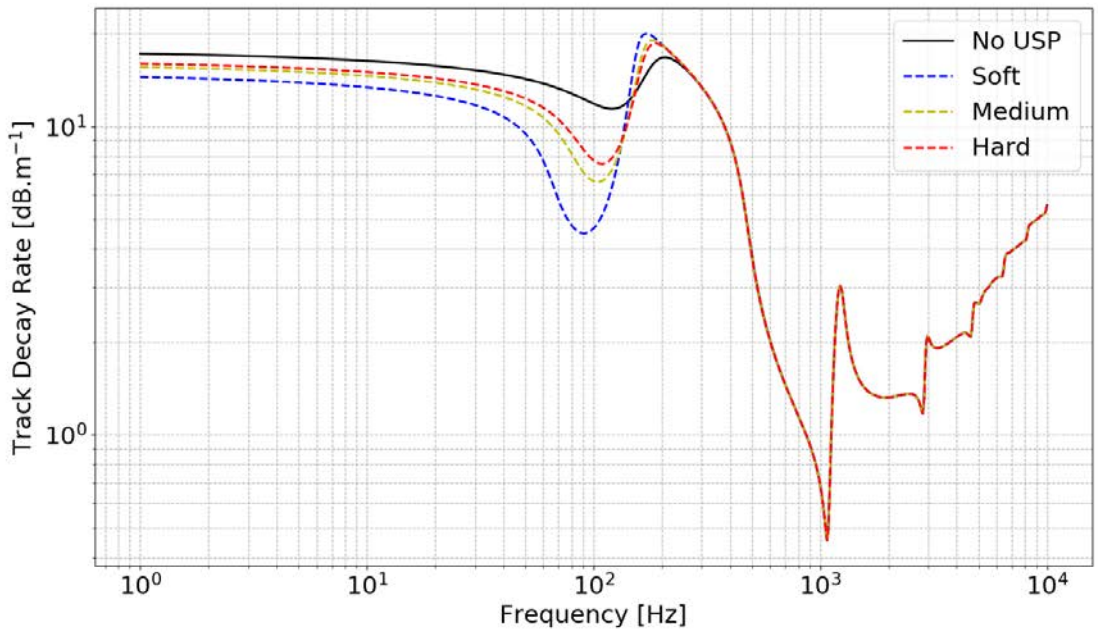

Figure 15 – Comparison of the three selected USPs using the spring/mass model

However the resulting drop in TDR is greatly underestimated compared to what can be simulated with the new track model (Figure 16).

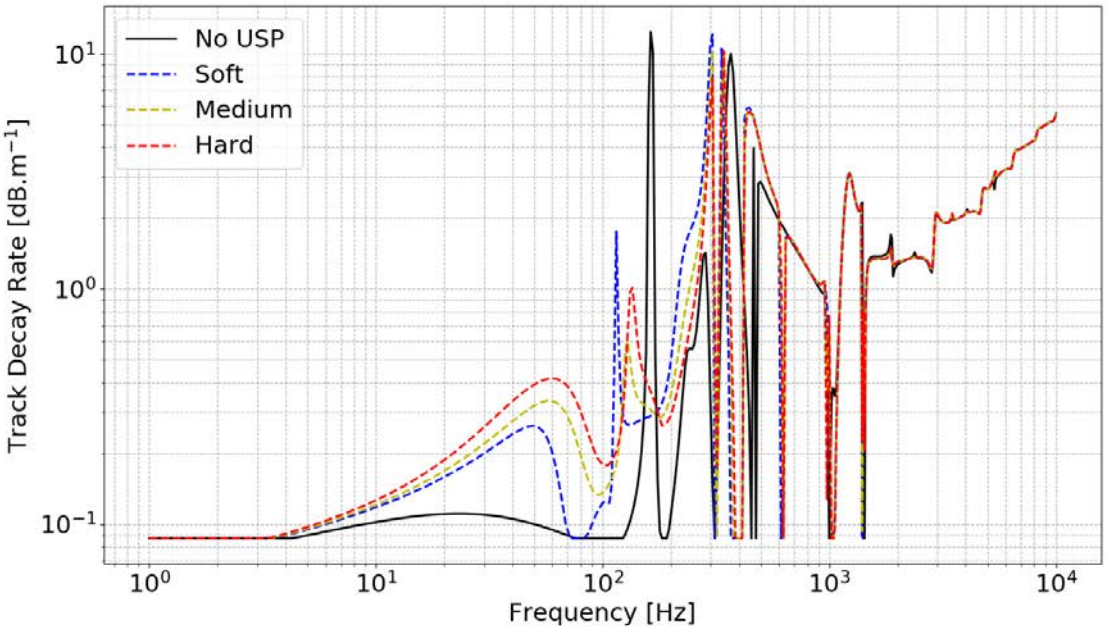

Figure 16 – Comparison of the three selected USPs using the supported sleeper model

One measurable effect of installing USPs on a track line is the increase/decrease of sound emission/TDR. This feature is represented by the state of art model (Figure 15) but is slightly different with the new model: the simulation without any USP shows the lowest TDR while it is expected to give the highest. In the same time, simulation including USPs show an increase in TDR for stiffer pads, which fits with the expectations. These observations thus suggest a possible issue with the ballast properties used in the new model.

In Figure 17, the same simulations as in Figure 16 are done, the only difference being that the ballast loss factor is lowered from 1.0 to 0.1 (now same value as the USPs loss factor). This time the expected order is respected: a track without any USPs gives the best/highest TDR while a track with USPs gives a lower TDR value as the pad stiffness decreases. This suggests that a ballast loss factor of 1.0 is too high to represent correctly the properties of ballast. This value was taken from the state of art spring/mass model. In this case a high damping in the ballast was required to create energy dissipation at the boundaries. In the case with supported sleepers, where the whole length is represented, the loss factor doesn't need to be so high to achieve enough dissipation. An exaggerated ballast loss factor is even shown to result in unrealistic response. More investigation on a correct range for this parameter should be done, until then the value should be kept low enough to re-

spect the TDRs order (No USPs > hard USPs > soft USPs) and the simulation of a track without any USPs can be used as a reference to verify this condition.

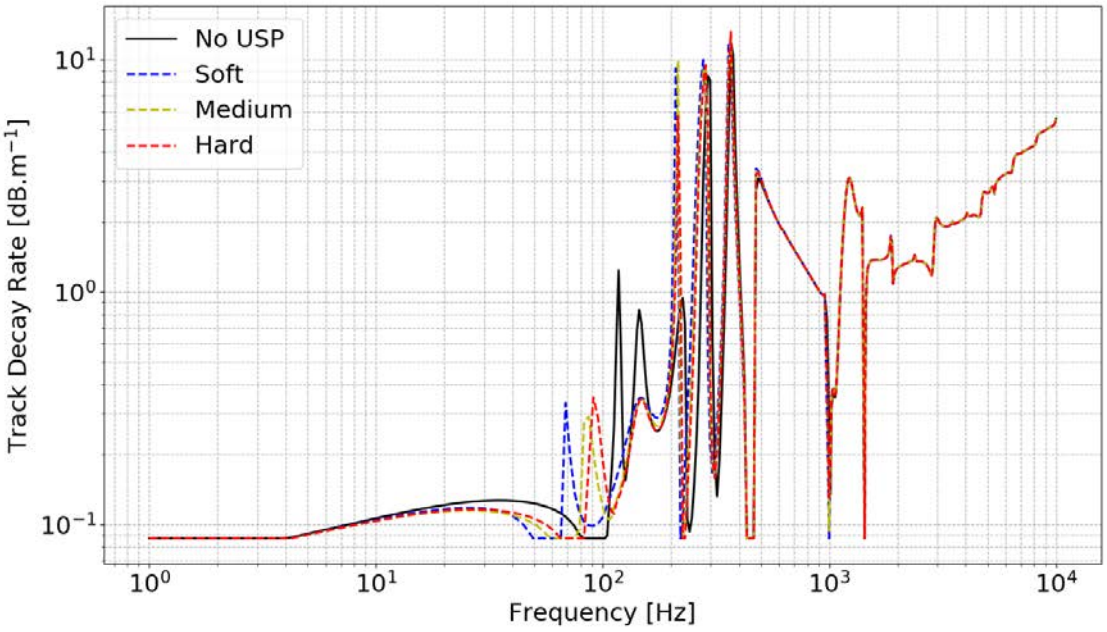

Figure 17 - Comparison of the three selected USPs using the supported sleeper model, same loss factor for ballast and USPs

To conclude on the accuracy of the new track model, the TDR measured during the Ef-fretikon campaign is shown in Figure 18. The starting level of the TDR under 10Hz, its ramping behaviour and oscillations until the cut off and finally the resonances of the track after cut off, all this features are now captured by the track model. Some more parameter fitting, especially to account for the temperature and pre-loads on the rail pads, USPs and ballast, is required but the model already allow a great numbers of observed behaviours to be simulated, especially considering the lightness of the model in term of calculation time.

Regarding the module 3 and its deliverables:

- A sleeper model has been implemented, validated with experiments and is fully working in its current state.
- The connection to the track model is done and also fully working in its current state.
- Simulating the influence of the USP type over the track dynamic, including the sleepers is now achievable and has been done for the current USP selection from SBB
- Module 3 is considered done

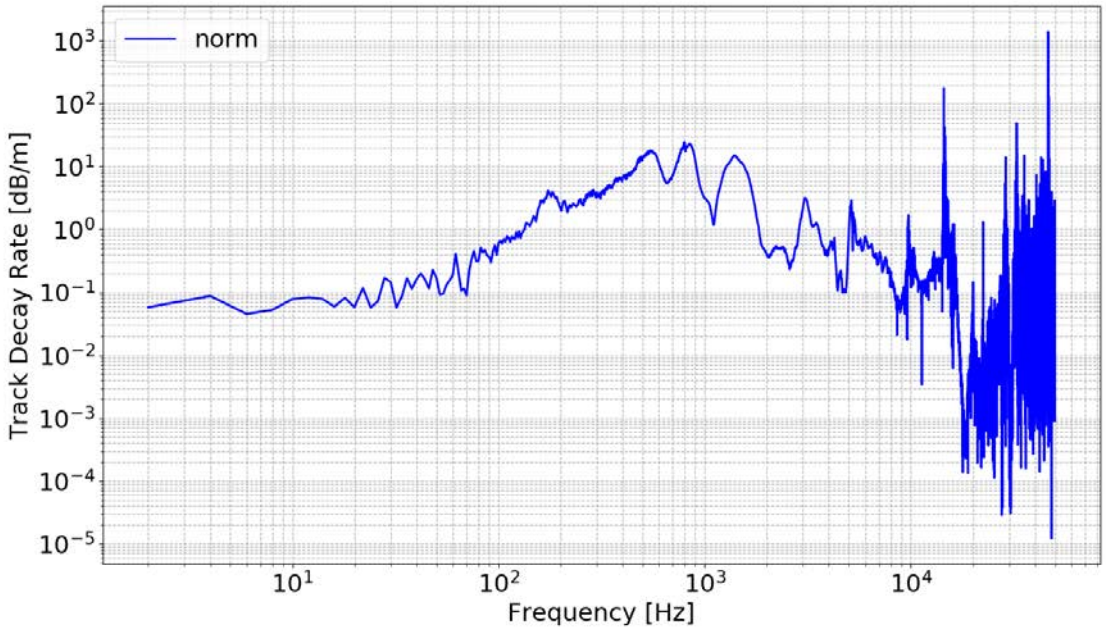

Figure 18 – TDR measured during the Effretikon campaign

V - State of art noise emission estimation (Module 5)

The estimation of the total sound power radiated by the rail is calculated thanks to an extension of the track dynamic model which can be found in [2]. The rail is approximated by an oscillating cylinder with a radius chosen to fit the emission of a Boundary Element model of the rail (done in [2] for a UIC 90 rail, with an equivalent cylinder radius of 54mm). In this state of art technique, the rail vibrations are calculated under the assumption of an Euler beam instead of Timoshenko, which represents a step backward for the track model in use. In [2] this assumption allows the sound power to be calculated easily and at the moment no work is found in the literature to extend this approach to Timoshenko beams. For the current report this state of art approach is applied as it already gives information about the effects of USPs on noise emissions. For the next 3 months period of the project, one task will be to extend this approach to a track model with Timoshenko beams but also with supported sleeper to take advantage of the new developments presented in section III and IV of this report.

Figure 19 shows the radiated sound power level in dB for the same track either with or without USPs. In the case with USPs, the three pads selected by SBB are tested separately.
As expected from the results of section IV on TDR (stiffer USPs results in higher TDR), Figure 19 shows that the sound power emitted is lower when hard USPs are used (at best 3dB

lower from 1Hz to 60Hz) or even better if no USPs are used. Since USPs main purpose is ballast protection and not noise emission, the latter observation should only be used for comparison, not as an optimal solution.
Due to the use of mass/springs for the sleeper and ballast, the results of Figure 19 miss important features in the low frequency, as the low TDR values and the sleepers resonances are not taken into account. As a first step to implement the model from [2] this is however a good place to start and a good basis to develop upon for the rest of the project.

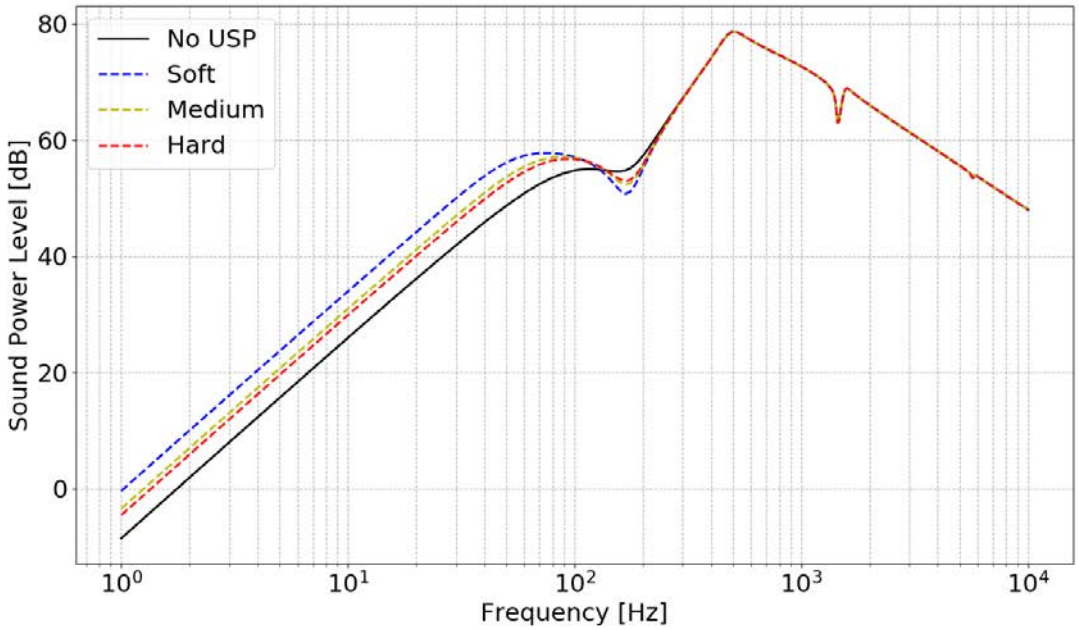

Figure 19 – Sound power radiated with or without USPs

Improvements for this method will include:

- Using a Timoshenko beam instead of Euler to model the rail (Pin-Pin resonances)
- Use supported sleepers instead of mass/springs model
- Use contour integration to calculated the sound power instead of analytical derivations to allow the two previous points to be included in the radiation model

It has to be remarked that the two first points are already ready since project modules 2 and 3 are achieved. Only the third point needs to be implemented to complete the model and allow the connection of the detailed track dynamic to the track acoustic.

VI – Conclusions, Update and Budget

Conclusions for the current report:

- Module 3 and 4 have been re-arranged to optimize the work load and objectives
- Material data from GETZNER are available to validate our own measurements when done, and meanwhile the GETZNER documentation is used to describe the USPs properties
- A supported sleeper model has been implemented and validate by comparison with measurements
- The track model now use supported sleepers instead of mass/springs which represents the achievement of module 3.
- A model for sound radiation has been implemented and used to access the influence of the type of pads over the emissions

Update on project modules, at the 5th April 2019:

Modules	State	Comments
1		Delay due to DMA availability, scheduled and not limiting
2		-
3		-
4		Starting next phase
5		Radiated sound power levels implemented
6		Sleeper Measurements done
Reporting		6 months report written, next one for 9 months

Labels:

Done	In progress – On time	In progress - Delay

Update on project budget, at the 5th April 2019:

Labels	Budget [CHF]
Salary 50% Post Doc – 6 months	25375
Sleeper Measurements Expert	4300
Project Management (5%) – 6 months	1626
Total	31301
Remaining from project budget	37001

VII - References

1. *Railway Track Noise Emission – Influence of Under Sleeper Pads on Railway Rolling Noise Emissions, Project Proposal.* B. Morin, 2018, Empa.
2. *Railway Noise and Vibration: Mechanisms, Modelling and Means of Control*. D. J. Thompson, Elsevier 2008.
3. *Sylomer Schwellenbesohlung SLB 2210 G*. Getzner Werkstoffe GmbH.
4. *Sylomer Schwellenbesohlung SLB 3007 G*. Getzner Werkstoffe GmbH.
5. *Sylomer Schwellenbesohlung SLN 1510 G*. Getzner Werkstoffe GmbH.
6. *Dynamic modelling of concrete railway sleepers*. S.L. Grassie. Journal of Sound and Vibrations, 187, 799-813, 1995.
7. *Analyses of lateral vibration behaviour of railway track at high frequency using a continuously supported multiple beam model*. T.X. Wu and D.J. Thompson. Journal of the Acoustical Society of America, 106, 1369-1376, 1999.
8. *Data Sheet Overview Sylodyn*. Getzner Werkstoffe GmbH.

Empa
Materials Science and Technology

Rail Track Noise Emission
Influence of Under Sleeper Pads on Railway Rolling Noise Emissions

Technical Report – 9 Months

Laboratory for Acoustics and Noise Control

Empa
Überlandstrasse 129
8600 Dübendorf, Switzerland

Dübendorf, 2 July 2019

Dr. Benjamin Morin

Project Reference: O315-0323
Empa Number: 5211.01578.100

Zusammenfassung

Der vorliegende Bericht fasst die erzielten Ergebnisse zusammen, welche in den dritten drei von insgesamt zwölf Monaten Projektdauer erarbeitet wurden.
Im ersten Teil des Berichtes wird ausführlich über die Charakterisierung der Materialeigenschaften von Schwellenbesohlungen von Getzner (DMA Messungen an der Empa) und die nachfolgende Modellbildung der Materialmodelle berichtet. Der zweite Teil beschreibt den aktuellen Stand der Modellierung des Oberbaus. Der Entwicklungsstand und die Vor- bzw. Nachteile der beiden Modellansätze wird erklärt. In einem dritten Teil wird die Strategie zur Berechnung des vom Oberbau abgestrahlten Luftschalls dargestellt, welche schliesslich einfach zu implementieren und doch hinreichend genaue Resultate liefern wird.
Schliesslich werden im Bericht sowohl ein aktualisierter Zeitplan als auch eine Budgetübersicht dargestellt.
Die verwendeten Referenzen sind am Schluss des Berichtes aufgeführt.

Summary

This report resumes the third period (months 7-9) of the project *Rail Track Noise Emission - Influence of Under Sleeper Pads on Railway Rolling Noise Emissions,* as set in the project contract.
The document starts with a detail of the first set of material characterization performed at Empa and gives an assessment of the measurements quality. The full spectrums of the materials properties are derived and viscoelastic identification is investigated.
The second part of the document treats the modelling of track lateral vibrations and a model is implemented based on the literature. Comparison between the reference and the model is done for validation purposes and to determine the required corrections.
The third section gives information about the next phase of the project and how the noise emission calculation will be dealt with.
Finally, schedules and budget are updated and the report ends with a reference section.

Table of content

I – Material characterization of GETZNER's USPs

Samples from three types of USPs (SLN1510, SLB1510, SLB2210) have been shipped to Empa by Getzner. Samples from SLB3007 pads were missing in the first shipping and have since been received but not tested yet.
The samples are all made of polyurethane foam and their characterization is done through Dynamical Mechanical Analysis (DMA) [1]: the samples are tested in tension or compression at multiple frequencies (limited by the machine specifications and resonances) and multiple temperatures (limited by the machine specifications and samples glass transition/melting point). Based on the measurements, Time-Temperature Superposition (TTS) [2] is applied to obtain full spectra for both storage and loss modulus instead of the machine limited frequency range (here from 0.1Hz to 100Hz).
The measurements detailed in this section represent a first attempt at USPs material characterisation: the aim was to get used to the use of the DMA at Empa and test its capacities/limit to ensure accurate measurements later. The glass transitions and melting points of the different materials were also investigated to define proper measurements conditions.

In the first part of this section, the example of the SLB2210 is given: storage and loss modulus measurements are detailed, as well as a quality indicator graph. Then a resume of measurements and quality is given for all materials.
The second part explains how the TTS is applied on the example of the SLN1510 and the master curves of all materials are given and commented.
The last part deals with the modelling of the master curves with viscoelastic models.

1) Results of the measurements

The measurements data for the SLB2210 are given in Figure 1 and Figure 2. Two main trends (both expected for viscoelastic materials) can be observed:

- The storage and loss modulus increase with the frequency.
- They both decrease when the temperature augments.

The following comments concern the measurements quality:

- At the lowest temperatures, the low frequency measurements are noisy (clear on Figure 2). This is due to the fact that at low temperature the material gets stiffer, especially close to its glass transition temperature. With such an increase in stiffness, the measured displacement may reach the order of magnitude of the machine sensitivity, thus resulting in poor measurements quality.

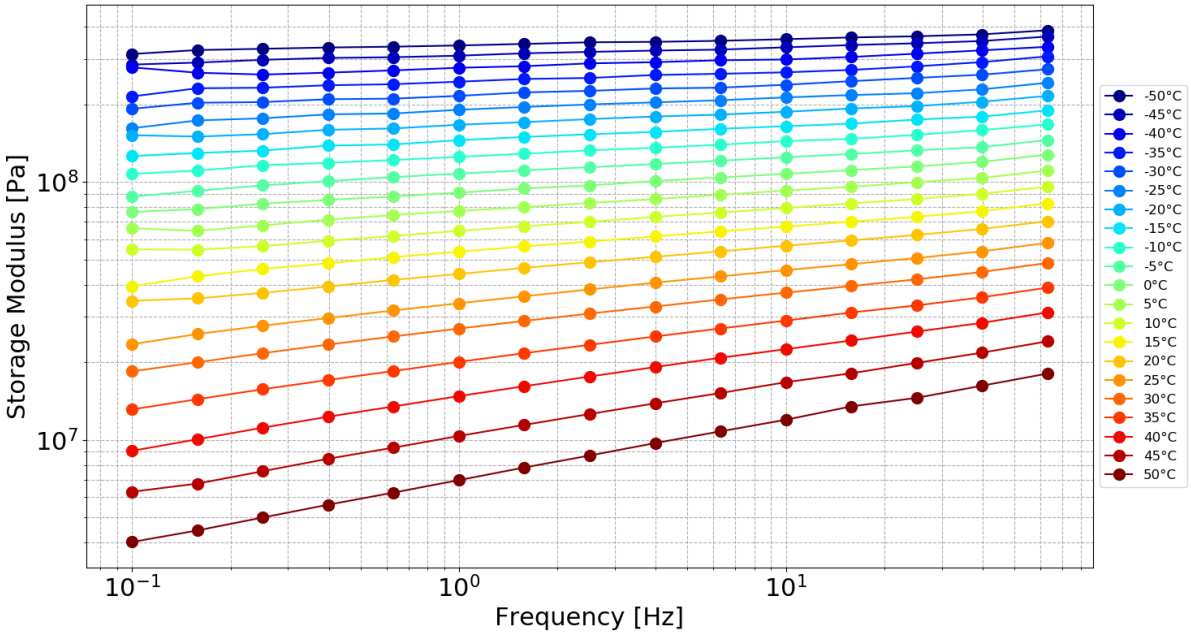

Figure 1 – Measurements of the SLB2210 storage modulus

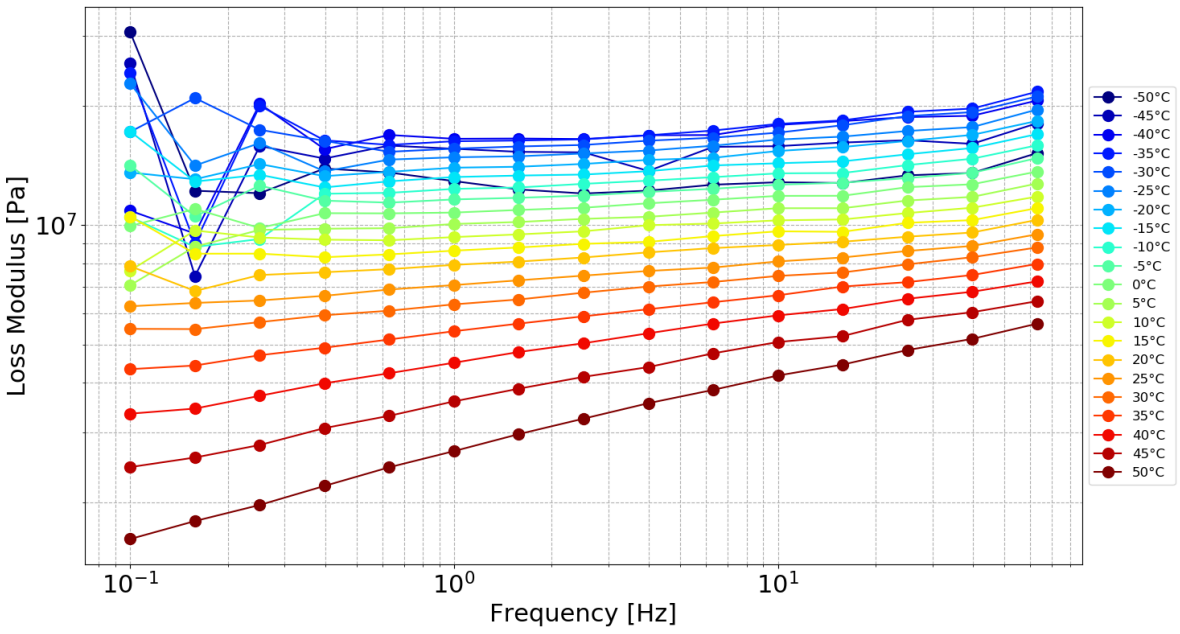

Figure 2 – Measurements of the SLB2210 loss modulus

- A good way to determine which temperature to keep after measurement is to look at the spacing between isotherms (points at same temperature). On both Figure 1 and Figure 2 it can be seen that the high temperatures isotherms are still well-spaced which indicates that more measurements at higher temperature could have been performed and will maybe be missing for the TTS and viscoelastic identification. On the other hand at low temperatures the isotherms get closer to each other indicating that the low temperature limit (glass transition) is almost reached.

A better way to assess the quality of DMA measurements, instead of just looking at the modulus isotherms is to plot the Cole-Cole graph (Figures 3-5). Ideally this would look like a deformed top half circle. This 'semi-circle' would be assembled from the continuous alignment of isotherm arcs, from high temperatures/left to low temperatures/right. However in reality Cole-Cole graphs always exhibits divergences from the ideal case and the possible issues with the measurements can then be determined graphically.

For the SLB2210 (Figure 3), the first observation is that the graph is only a quarter of 'circle', starting around the top point and describing a 90° angle when counting clockwise. This indicates that more measurements at higher temperatures are required, which would give the missing quarter circle of the left. That was already pointed out by the spacing of the high temperature isotherms on Figure 1 and Figure 2. However the Cole-Cole graph gives more information as it gives an indication on the desired max temperature: here almost the whole quarter circle comes from measurements between 0°C and 50°C, so the missing quarter could probably be obtained by measuring between 50°C and 100°C.
Figure 3 also shows that at lower temperatures (starting around 15°C), some of the low frequency measurements (left side of each concerned isotherm) are not well aligned with the rest of the points. This was already pointed out on Figure 2 and comes from the increasing stiffness of the samples at low temperature and the sensitivity of the machine.

Looking at the SLB1510 (Figure 4), the same issues as for SLB2210 shows up, which can be expected since both materials are from the same type (SLB), only with different porosity. To summarize: the temperature range should be extended to higher temperatures, and under 15°C the low frequency measurements should be removed.

Finally, for the SLN1510 (figure 5), an almost ideal case of Cole-Cole graph is obtained. A few observations can still be made:

- Above 5°C-10°C the material is already close enough to its melting point to have deteriorated properties. This is shown by the superposition of the isotherms.
- At low temperature (starting from -20°C), some of the low frequency measurements should be removed as they don't align with the rest of the points. For SLN1510 this is

however way better than for the SLB materials since the number of measurements to remove is negligible.

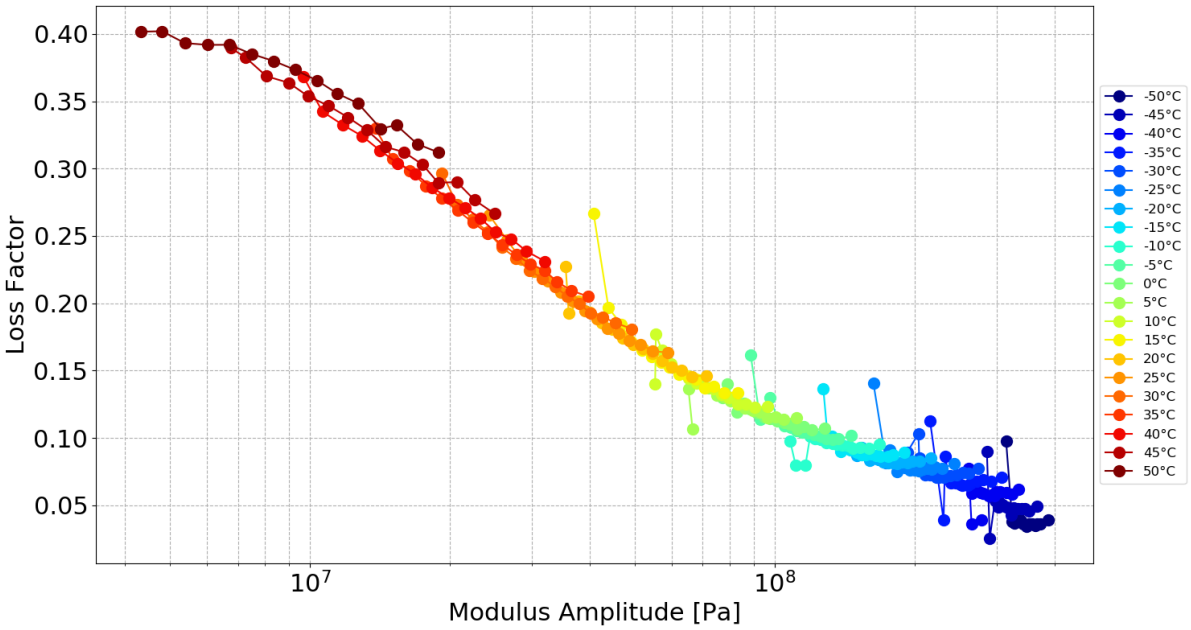

Figure 3 – Cole-Cole graph for the measurements of the SLB2210

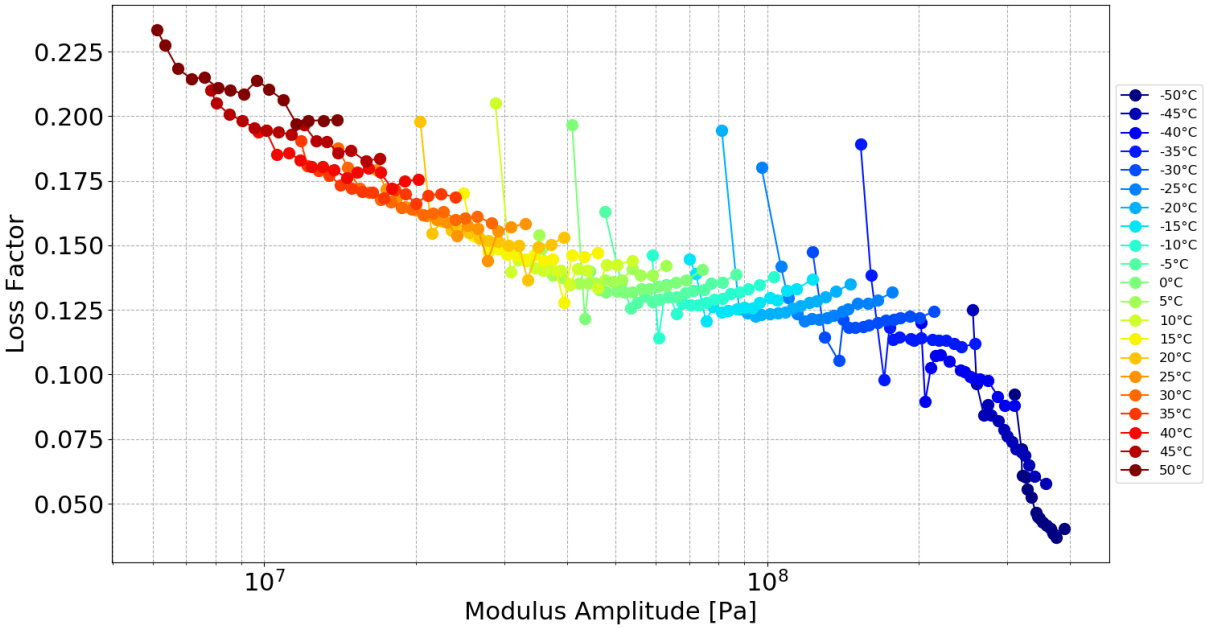

Figure 4 – Cole-Cole graph for the measurements of the SLB1510

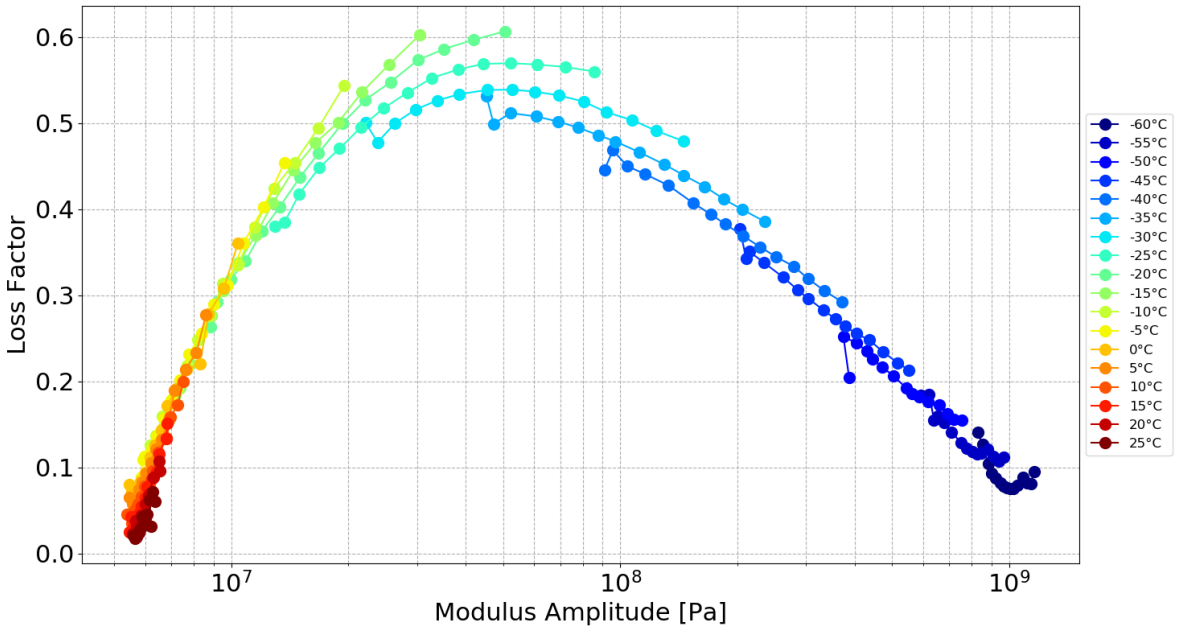

Figure 5 – Cole-Cole graph for the measurements of the SLN1510

To conclude on the DMA measurements quality, one should use the Cole-Cole graphs to check if the temperature range needs to be extended/shortened and check if frequency points need to be removed on certain isotherms.
For the current report TTS will be applied directly to the measurements already performed even if they would need to be extended as shown in this sub-section. This is due to the difficulty to access the machine. Now that the materials and machine are well known a second test campaign will be performed to ensure the best measurements quality possible. This second set of measurements will be used for the final model in this project.

2) Time Temperature Superposition

The TTS is applied to all previous measurements following the standard ISO 18437-6 [2]. The idea behind this method is to estimate the horizontal shift needed to get two consecutive storage modulus isotherms to superpose as best as possible, while selecting one isotherm as the reference. The shift is equivalent to apply a transformation to the measurements frequency, which results in an extended frequency range when applied to all isotherms. The final product of this method are the master curves of the material, namely complete (as close as possible depending on the measurements quality and machine specifications) spectra of storage and loss modulus.

Following ISO 18437-6 [2], the algorithm used to calculate the shifts is based on the projected area or overlap between two consecutives storage modulus isotherm as shown in Figure 6 and Figure 7. In the case where the TTS can be applied the area is quadrilateral and convex (Figure 6) while cases where TTS won't work can be detected from the cross quadrilateral shape of the area (Figure 7). One can then decide to keep or remove a temperature from the measurements based on these overlaps.

After applying this method to SLN1510, SLB1510 and SLB2210, only SLN1510 shows crossed overlaps above 0°C. This is due to the close proximity of the melting point, at least close enough for the material properties to start deteriorating. For SLB materials no crossed overlaps occur which indicates that all measured temperatures can be kept.

The master curves of these three materials for a reference temperature of 20°C are given in Figures 8, 10 and 12 for the storage modulus and Figures 9, 11 and 13 for the loss modulus.

As a reminder, for both SLB materials it has been observed on the measurements and Cole-Cole graphs that the temperature range should be extended to higher temperatures. This shows up on the storage modulus master curves where no horizontal plateaus exist at low frequency while the modulus should be constant under a certain frequency limit. This can affect the viscoelastic modelling process depending on which model is chosen. At high frequency the same observation can be made as no plateaus exist, although this wasn’t pointed out by the measurements and Cole-Cole graphs. This is due to a bad combination of machine limitations and sample glass transitions.

For all materials it was also observed that some of the low frequency measurements should be removed at low temperature and this is clearly visible on all master curves, especially for all three loss modulus, as the curves become noisy in high frequencies (related to low temperatures via TTS).

Lastly, the deterioration of SLN1510 properties above 0°C are clearly visible on its loss modulus (Figure 13), which fits with the observations from the Cole-Cole plot (Figure 5). Isotherms above 0°C should be removed from the master curves.
Due to its material low melting point, SLN1510 should probably be kept for very specific track location with low temperatures all year long.

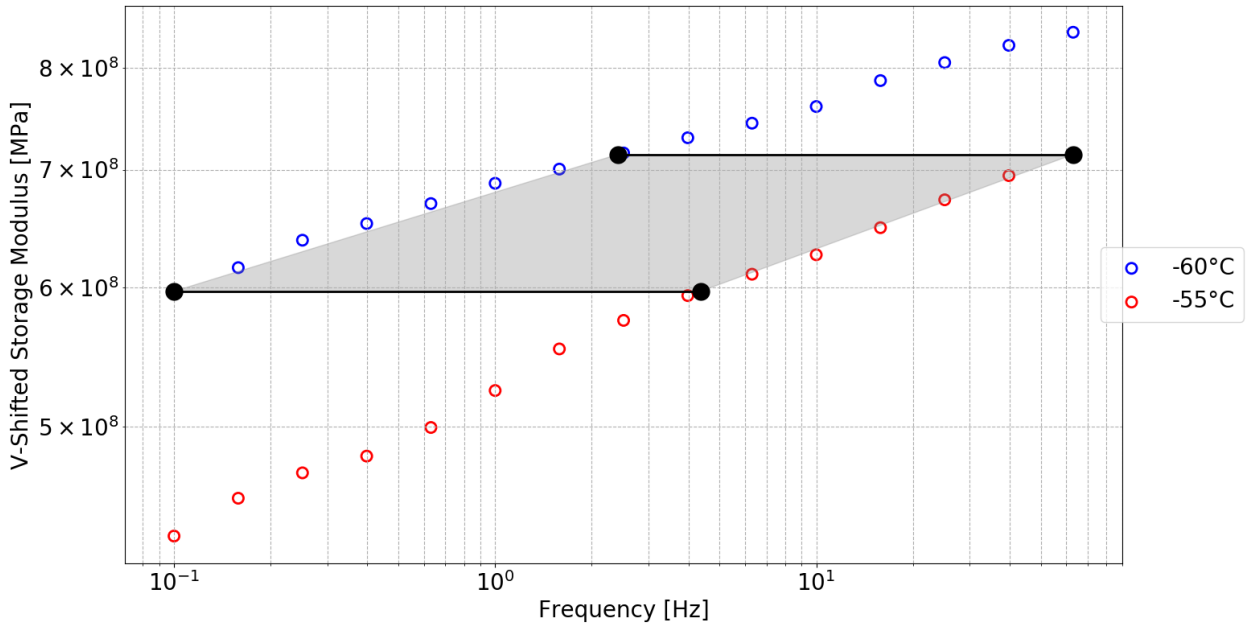

Figure 6 – Overlap between isotherms -55°C and -60°C of the SLN1510

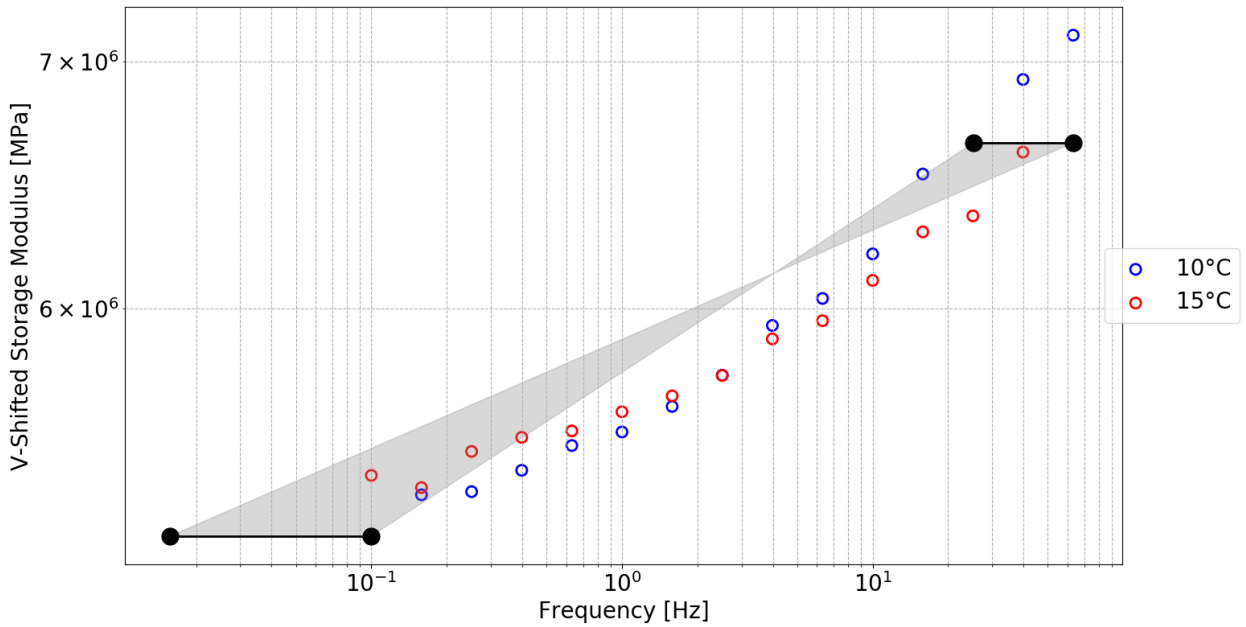

Figure 7 – Overlap between isotherms 10°C and 15°C of the SLN1510

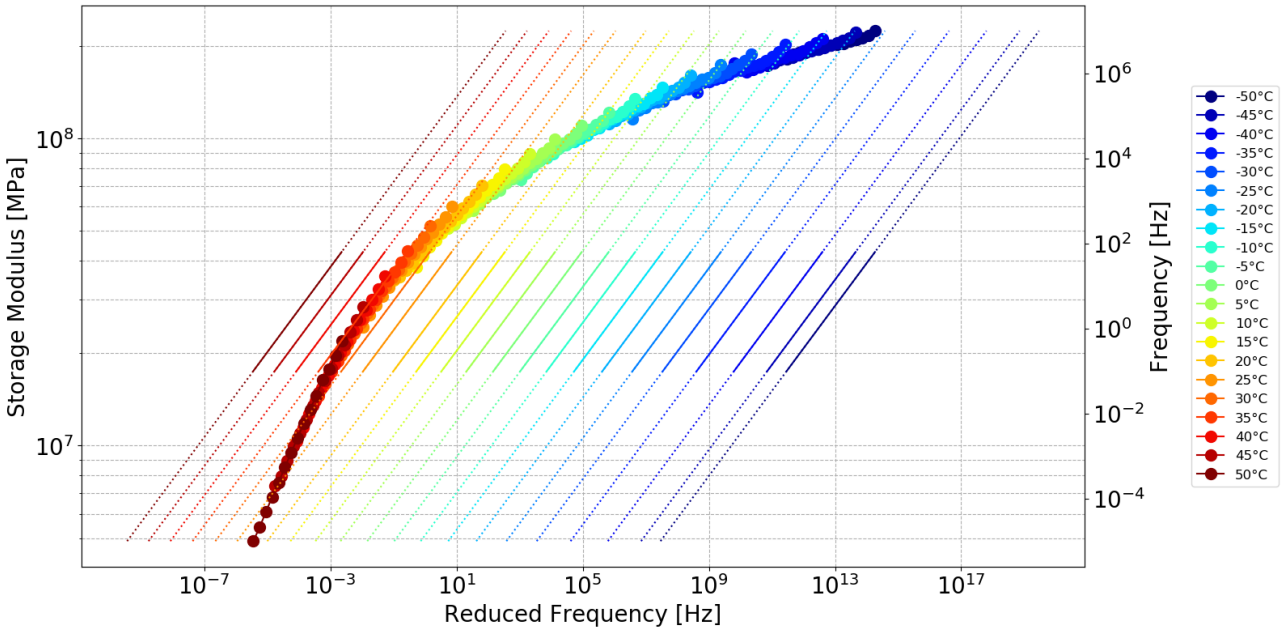

Figure 8 – Storage Modulus master curve for the SLB2210, at 20°C

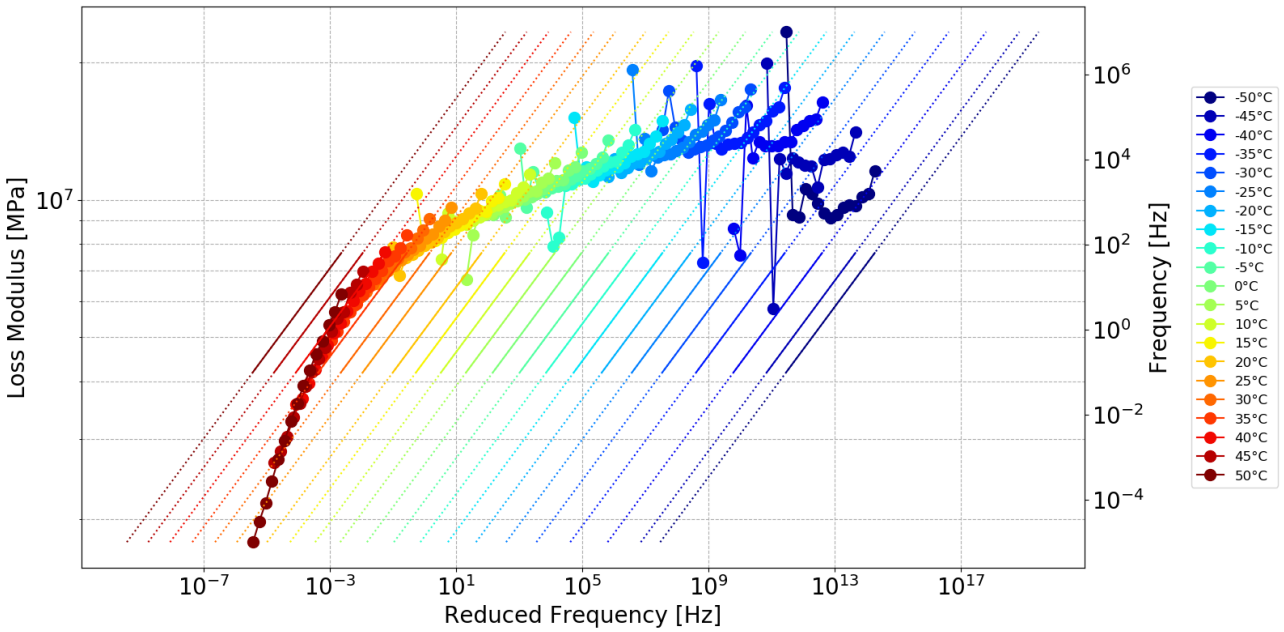

Figure 9 – Loss Modulus master curve for the SLB2210, at 20°C

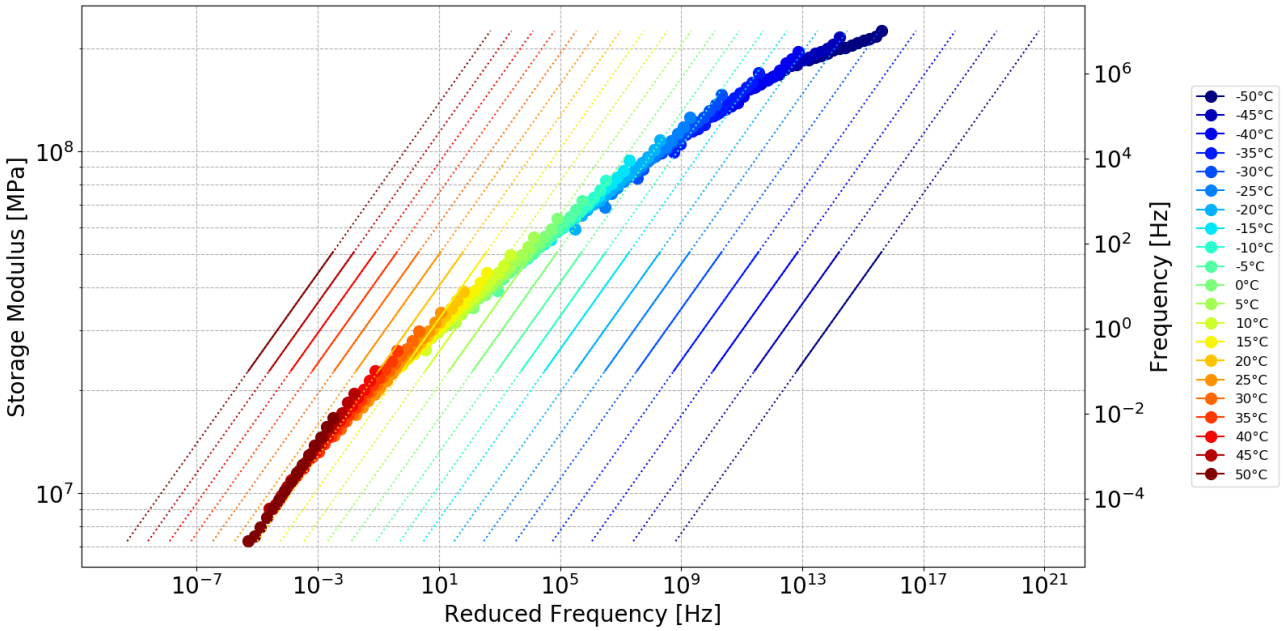

Figure 10 – Storage Modulus master curve for the SLB1510, at 20°C

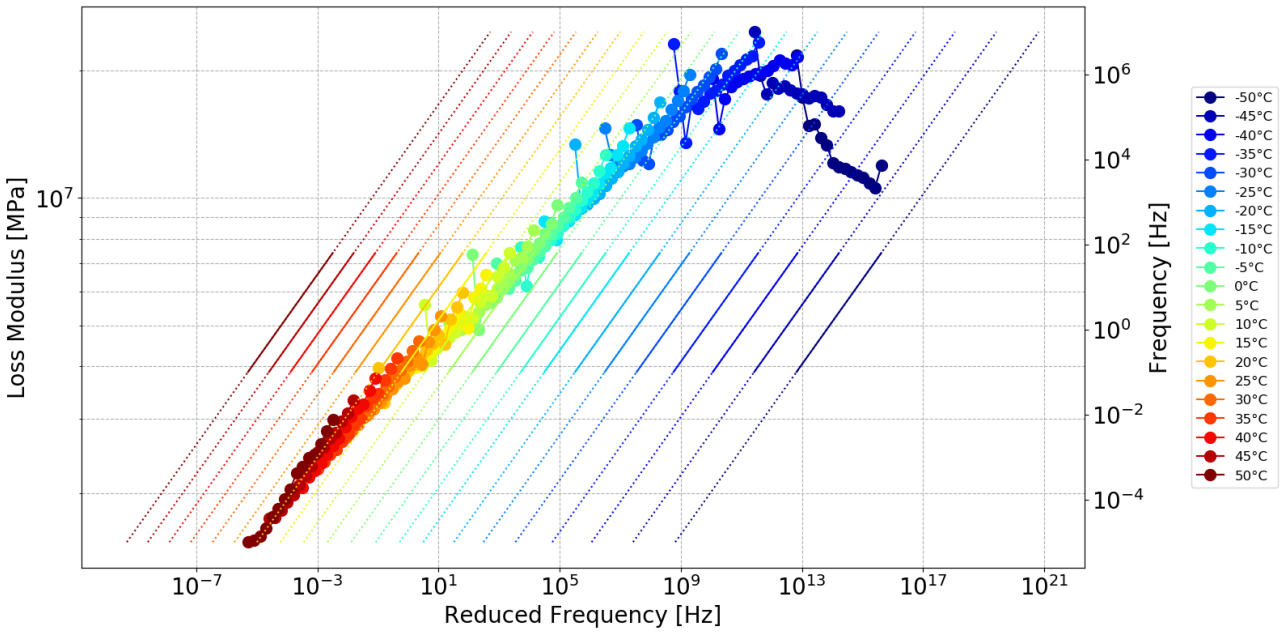

Figure 11 – Loss Modulus master curve for the SLB1510, at 20°C

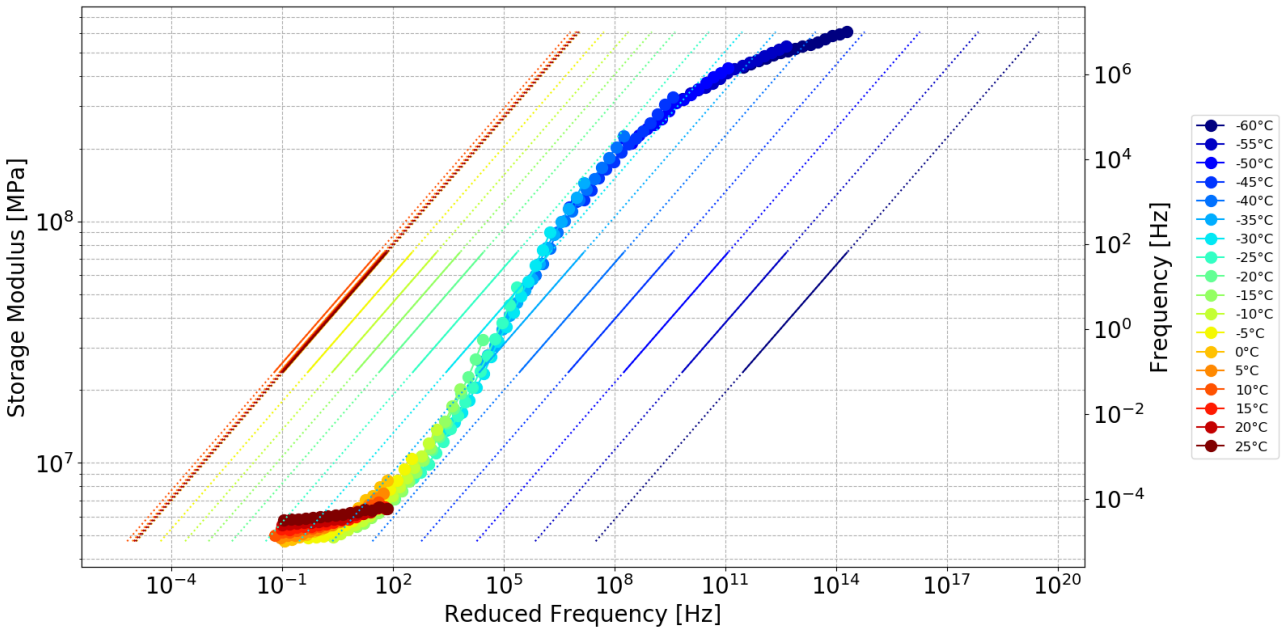

Figure 12 – Storage Modulus master curve for the SLN1510, at 20°C

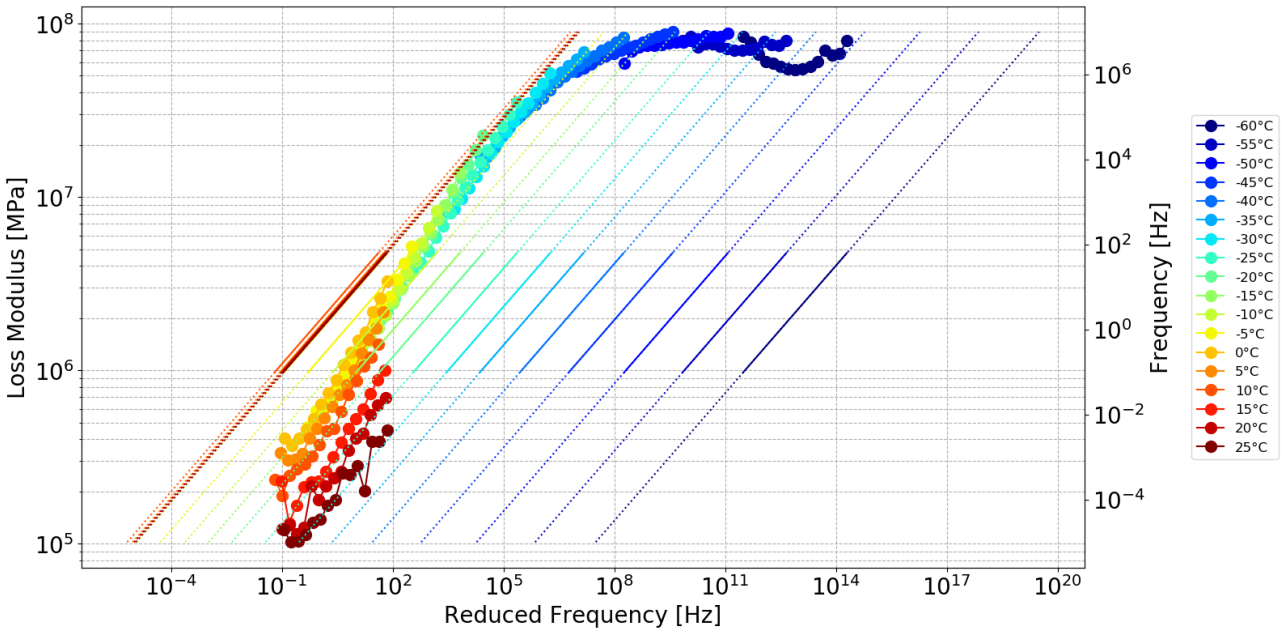

Figure 13 – Loss Modulus master curve for the SLN1510, at 20°C

3) Viscoelastic modelling

Based on the previous master curves, viscoelastic models are identified for SLN1510, SLB1510 and SLB2210. Two types of models are chosen:

- A fractional Zener (FZ) model, which depends only on 4 parameters.
- A generalized Maxwell (GM) model, with a number of parameters that depend on the desired accuracy.

The identification of the FZ is done very simply via graphical observations. The four parameters depend only on:

- The minimum and maximum plateau values of the storage modulus.
- The frequency of the maximum of the loss modulus.
- The slope of the storage modulus at the frequency of the max loss modulus.

The FZ models identified for all materials are shown in Figure 14. This type of model shows good predictions for the SLN1510 while both SLB materials can't be fitted properly. This is due to two main issues:

- The temperature range of the SLB measurements was shown during the quality assessment to not go far enough in high temperature. This leads to a missing plateau of the storage modulus at low frequencies, thus making it impossible for the models to start from the correct values.
- For low temperature measurements, SLB materials where almost at their glass transition and their stiffness made the measurements noisy. This makes it hard to properly define the maximum value of the loss modulus and the frequency at which it occurs. Also the temperature was not low enough to have a properly defined high frequency plateau as it can be seen that both storage modulus keep increasing.

In summary, the FZ model is able to fit the master curves for the SLN1510 but not for SLB materials, at least with the current measurements. If the temperature range is extended to higher temperature and if the low frequency measurements are cleaned up, then the FZ models could also fit SLB master curves.

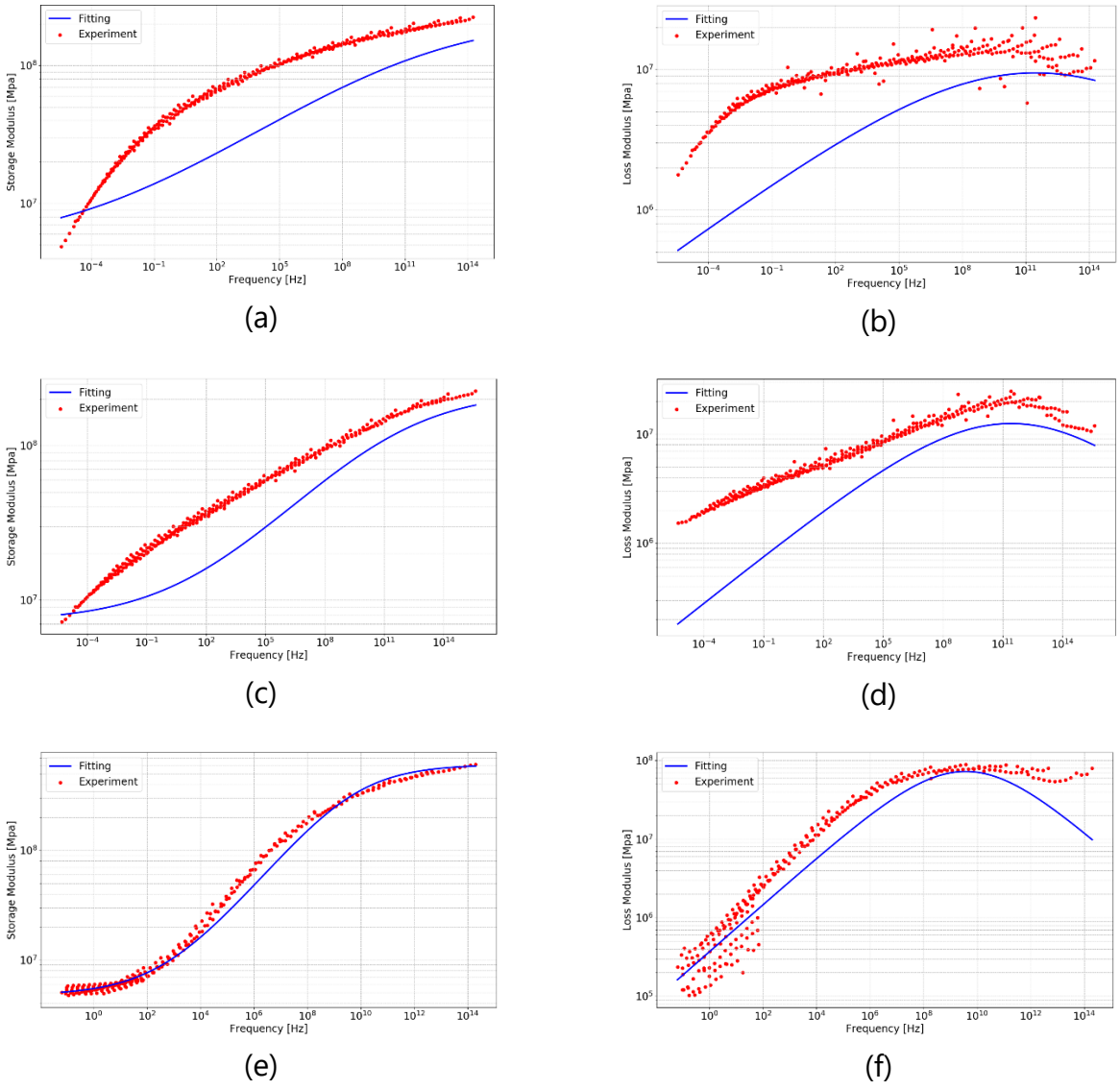

Figure 14 – Fractional Zener models for SLB2210 storage moduls (a) and loss modulus (b), SLB1510 storage moduls (c) and loss modulus (d), SLN1510 storage moduls (e) and loss modulus (f)

For the GM models the identification procedure is a bit more complex and relies on a numerical/graphical method applied to the storage modulus master curve [3]. To begin, two enclosing curves are drawn around the master curve. This enclosures are simply replicas of the master curves, shifted up or down. The example of the SLN1510 is given in Figure 15.
The next step is to draw a horizontal line starting at mid-level between the lower enclosure and the master curve, until it crosses the lower enclosure. The crossing point defines a zero. From this zero a diagonal line is drawn until it crosses the upper enclosure, which defines a pole. The method then goes on by drawing horizontal and diagonal lines until the whole master curve is spanned. Each resulting couple of zero and pole is then used to calculate the parameters of a Maxwell model (spring and damper in series). The final GM model is the association in parallel of all these Maxwell models.

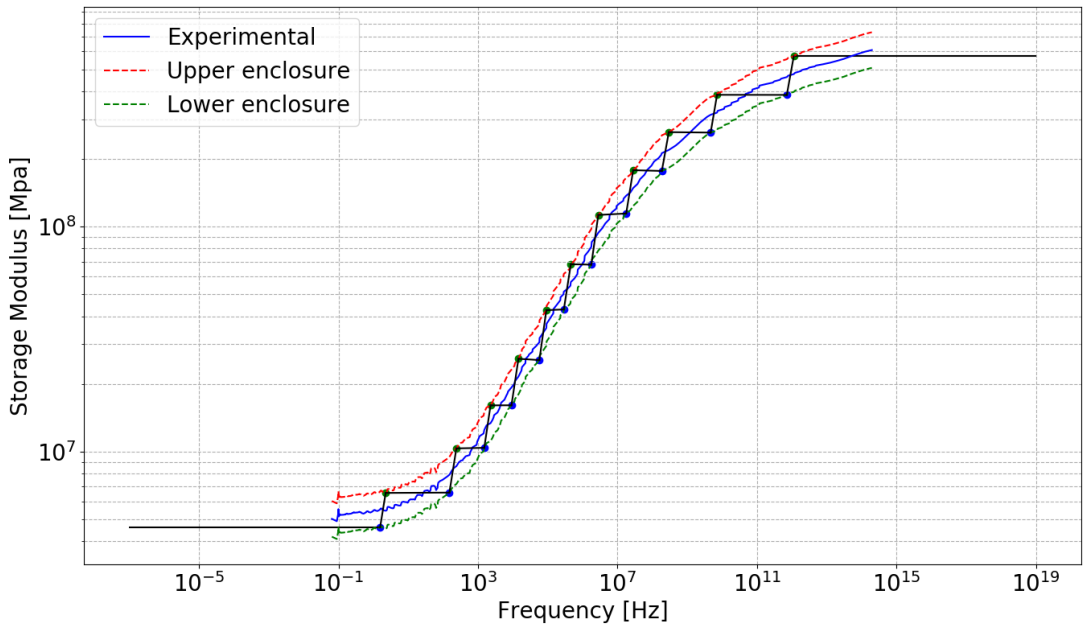

Figure 15 – Enclosure method applied to the SLN1510 storage modulus

The GM models identified for the SLN1510, SLB1510 and SLB2210 are shown in figure 16. Since all of these models are made of an assembly of smaller Maxwell models, their behaviour over the whole frequency range appears to oscillate. This is due to the fact that each Maxwell model covers a segment of the frequency range, each of them having their own slope and plateaus for the storage part and their own peak for the loss part.

The storage modulus fit for all three materials is acceptable for the frequency range that interest us (1Hz-10'000Hz) which represents an improvement compared to FZ models. On the other hand, the oscillations of the loss modulus for both SLBs are too extreme to make

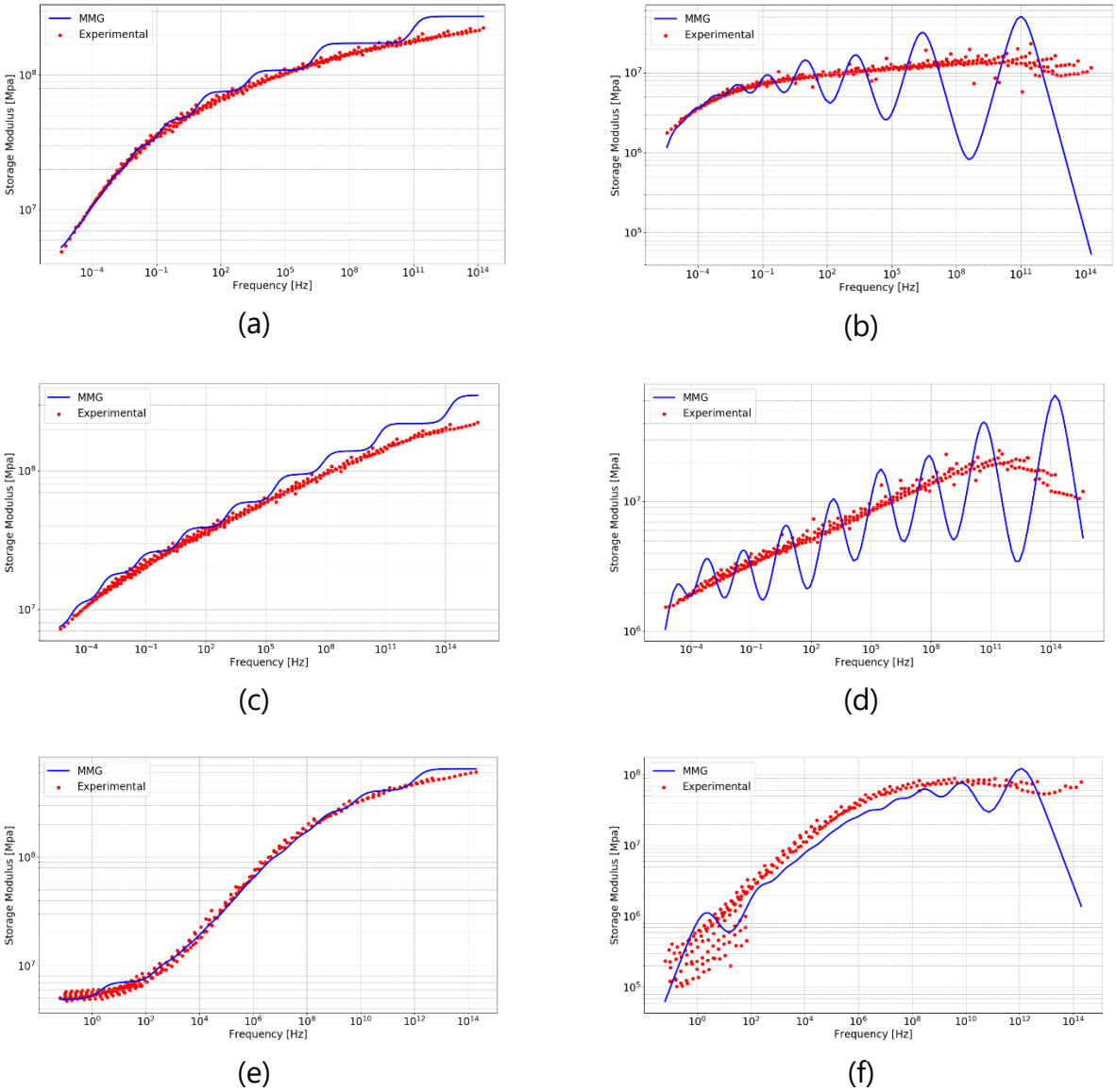

Figure 16 – Generalized Maxwell models for SLB2210 storage moduls (a) and loss modulus (b), SLB1510 storage moduls (c) and loss modulus (d), SLN1510 storage moduls (e) and loss modulus (f)

the models reliable in their states. For the SLN1510 the results of the fitting are good enough but a FZ model seems to be a better approach as it doesn't shows oscillations.

Summary:

The material properties of three polyurethane foam USPs from Getzner (SLN1510, SLB1510, SLB2210) have been measured via DMA at Empa.
DMA consists in measuring the complex elastic modulus at different frequencies and temperatures.
TTS is then applied to create a full spectrum of the complex modulus, also called master curves. The low temperature measurements are shifted to create high frequency values while high temperature measurements are shifted to create low frequency values.
From the Master curves, two types of viscoelastic models were identified.
For the SLN1510, a fractional Zener model is kept.
For SLB materials, the current DMA measurements don't allow for a correct viscoelastic fitting, their master curves are thus going to be used directly until a proper model is defined.

II – Lateral track behaviour modelling

The model chosen to represent the lateral motion of a track is based on the work of Thompson [4] and consists in representing the rail as a multi-body (figure 17):

- The rail head and foot are modelled as infinites Timoshenko beams.
- The web is represented by an infinity of beam elements

This type of model accounts for both bending and torsion of the rail as well as the coupling between the two. The supports are represented by continuous layers of mass and springs in series to account for the translational stiffness and by a continuous layers of spring for the rotational stiffness (Figure 17).

At the moment the model implementation is still in progress and two version exists:

- The first version (Model A) is an attempt to reproduce the state-of-art [4] and the current results come very close to the literature.
- The second version (Model B) is an attempt to extend the state-of-art [4] and create a new model for lateral track motion. The originality of this new model is to use discrete supports instead of continuous, at the cost of a large increase in difficulty. Also, since no similar approach is found in the literature, the validation of this model is sensitive.

For comparison, the acceleration transfer function of Model A and from the literature model [4] are given in Figure 18. The order of magnitude of both models fit well and Model A is able to represent the slope change between 100Hz and 200Hz. The differences come at higher frequencies as Model A peaks are sharper and also slightly shifted in frequency.

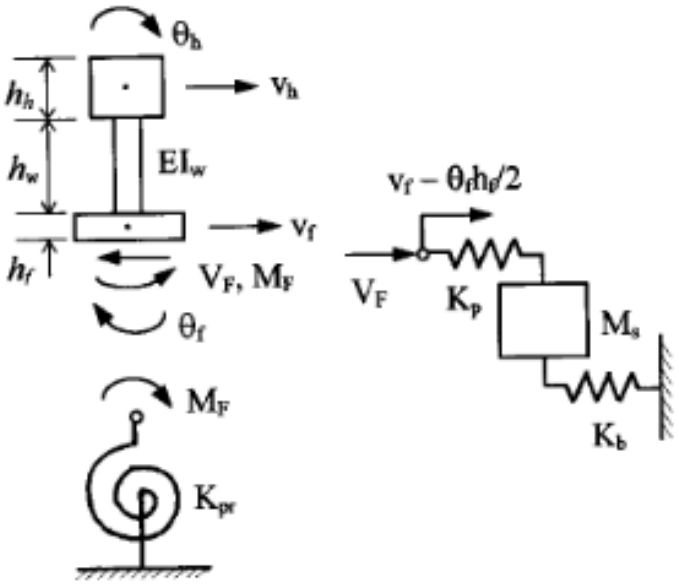

Figure 17 – Lateral track model based on three beams assembly, with support modelling

The same comparison can be done on TDR as seen in Figure 19. The TDR amplitude from model A is lower than the TDR from literature and the peaks in the high frequency region seem to be shifted. The peak amplitudes are not really comparable as the results from the literature are given in third octave bands, thus flattening any peak. However, Model A is able to represent the TDR's drop after 200Hz and its rise a little bit after 1000Hz. The wave-numbers from model A also fit very well with the ones from literature (wave I, II, III and IV on Figure 19).

Model A clearly needs to be corrected to better fit the literature. However, it still represent well some of the lateral TDR features, and its differences from the literature aren't too large to use it as a first estimate of USP stiffness influence on TDR.
Since the material characterization of the pads is still in progress, arbitrary values are chosen here (to be replaced with real values when ready): the TDR levels would be different with the real stiffness, but the differences between harder or softer pads are still visible.

As shown in the previous report, in the vertical case high/low USP stiffness are linked to high/low TDR, the best being reached when the USP stiffness is almost the same as the ballast stiffness. Here, the stiffness values are chosen arbitrary to be around the ballast stiffness at the hardest, and around 1/3 of it at the lowest. The results of this parametric study are given in Figure 20. As expected from the vertical case, stiffer USPs result in higher TDR values. This effect is also limited to the low frequency range.

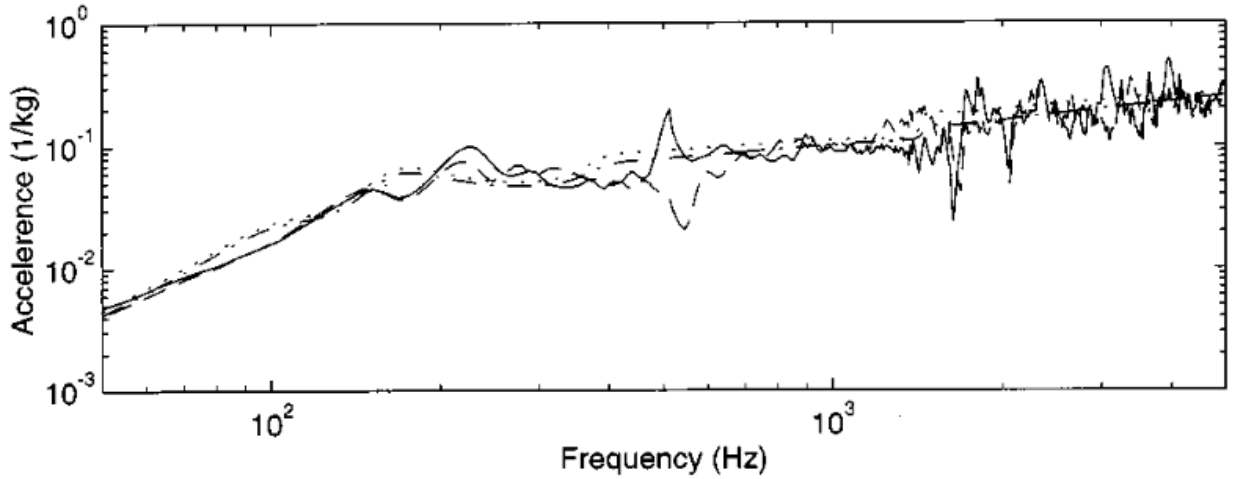

——— measured at mid span, --- measured above sleeper
-·-·- predicted at the center of head, and ··· predicted at the top of head.

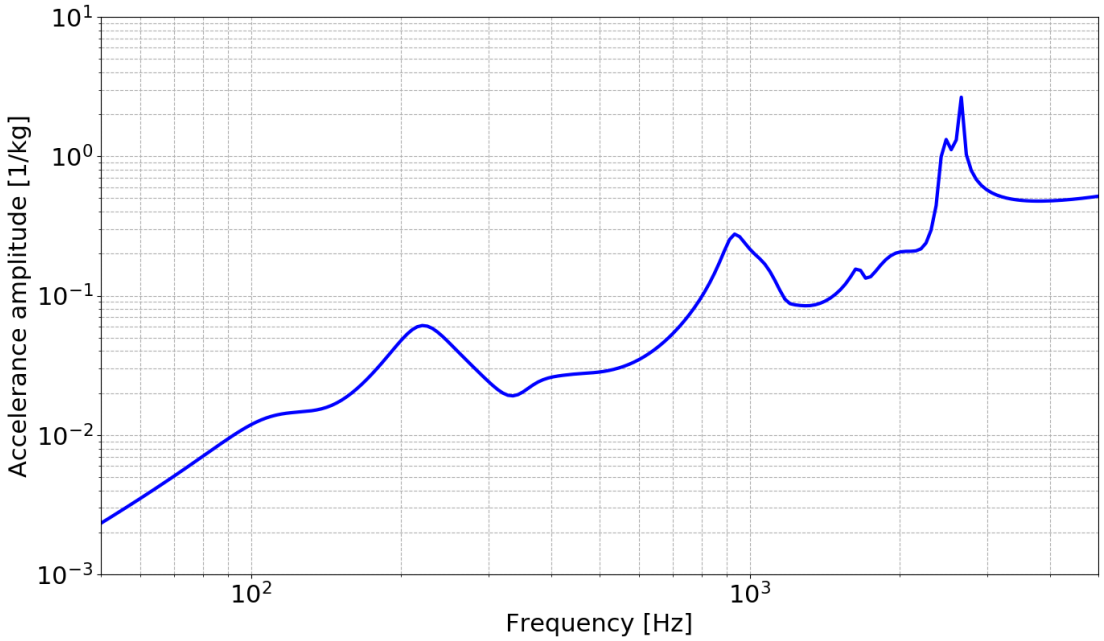

Figure 18 – Track accelerance for a lateral excitation, implemented model and literature [4]

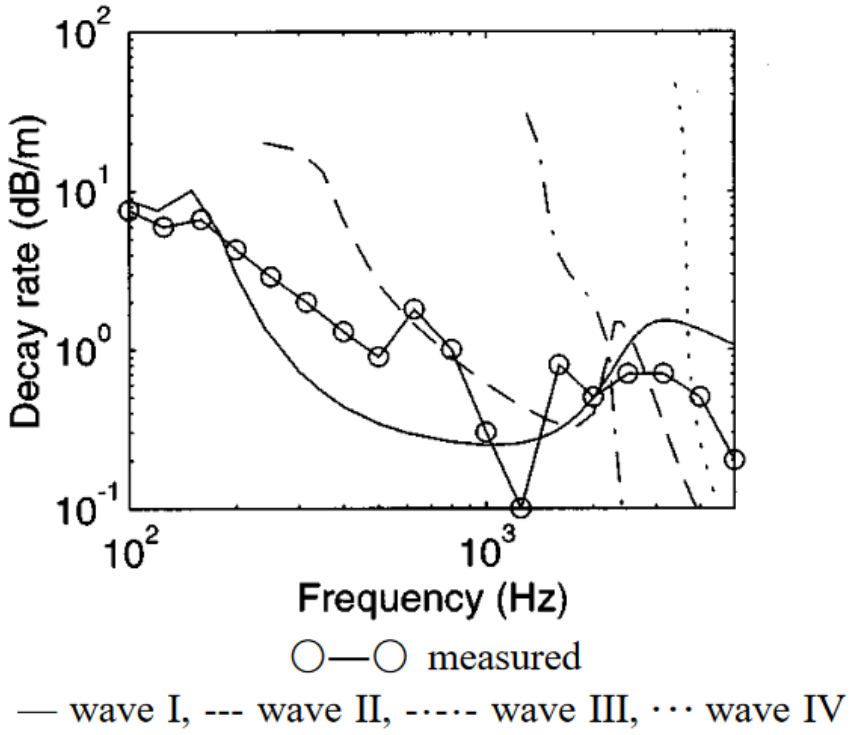

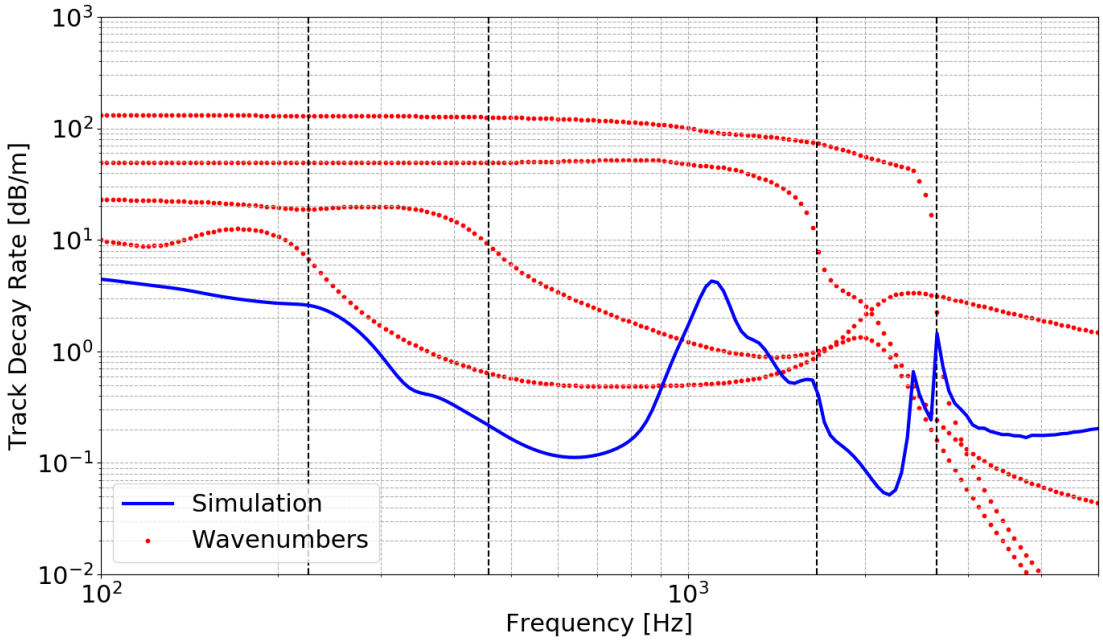

Figure 19 – TDR for a lateral excitation, implemented model and literature [4]

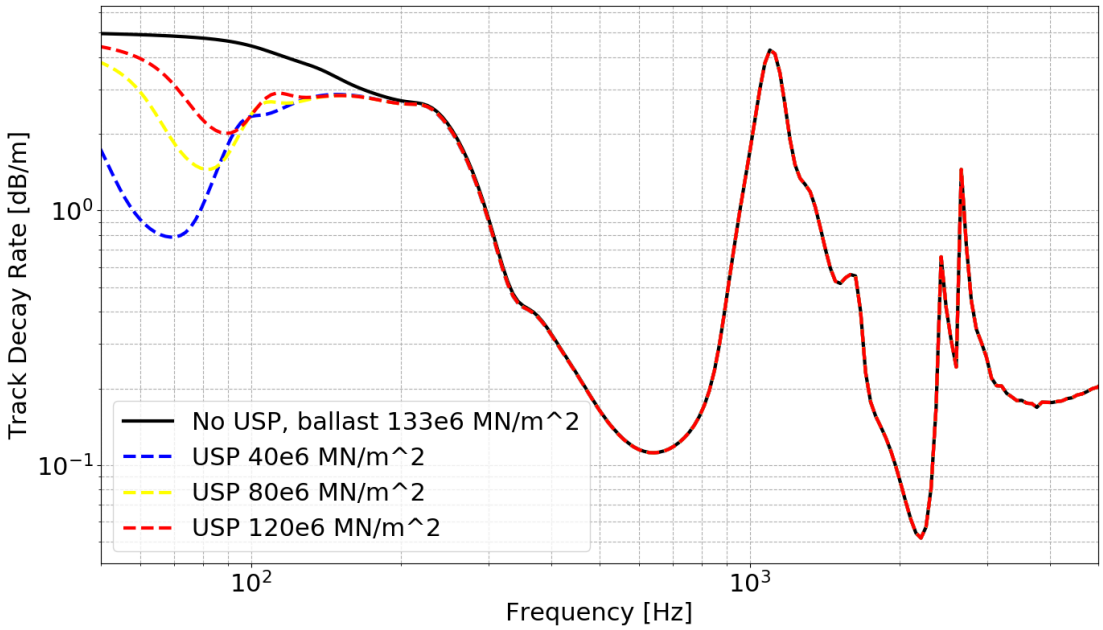

Figure 20 – USP stiffness influence on TDR for a lateral excitation

For Model B no results are shown in this report as a proper way to validate it isn't available yet. Its implementation is a lot more difficult than for model A and require more validation steps. In the vertical case, the difference between continuous and discrete support models tends to appear at mid-high frequency as the discrete models are able to simulate more details like pin-pin resonances. Thus model A, when validated, could be used to at least check the low frequency response of model B.

In the next few weeks of the project, the main priority will be to finish and validate models A and B. In order to achieve this goal, a first step will be to come back to the basics and use a simple continuously supported Timoshenko model. This model can be obtained from the vertical case for which it was already implemented. A Timoshenko model represents a simplification of model A and could be used to compare/validate model A low frequency response (as the model complexity decrease/increase the frequency range is more or less limited). Once model A is validated, model B can be compared to it and corrected as needed.

III – Noise emission calculation for next phase

Based on the track dynamics simulated with the models from modules 3 and 4, the radiated sound power W is calculated from the following integral:

$$W = \frac{1}{2}\rho_0 c_0 \sigma P \int_{-\infty}^{\infty} |v(x)|^2 dx$$

Where v(x) is the velocity of the rail in the lateral or vertical direction and x is the position along the rail.
In the previous report this integral was solved for a rail modelled as an Euler beam, following the approach of [5]. This technique is however limiting as Euler beam models of rails only represent correctly the low frequency range. In order to use Timoshenko beams, or even a 3 beams model in the lateral case, a new integration method must be defined.
This new method could be based on mathematical techniques to write the integral as a sum, but this would require time to be developed as no similar approach can be found in the literature.
An alternative would be to use numerical integration, by using the Simpson method for instance (Figure 21).

This kind of approach represent almost no difficulty to implement as it is well detailed in the literature and would still give very accurate results. Thus, in the next phase of the project the noise emission calculation will be done via numerical integration.

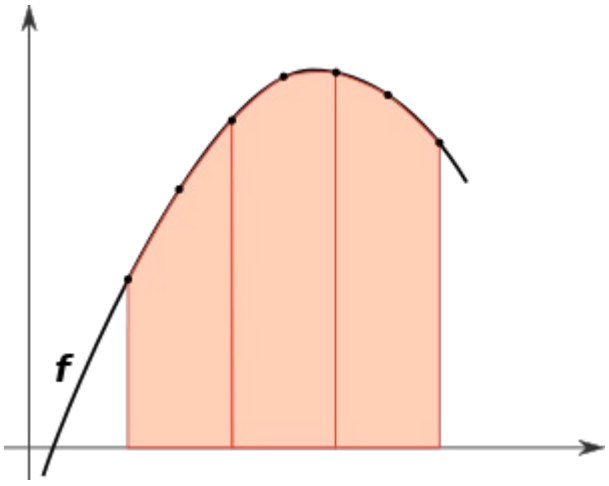

Figure 21 – Illustration of the Simpson integration [Wikipedia]

VI – Conclusions, Update and Budget

Conclusions for the current report:

- Module 1: Material characterisation with DMA finally started, the machine specifications have been tested on a few samples and the first set of results is ready. For both SLB materials it appears that more measurements should be done at higher temperatures. A second set of measurements will be performed to get full spectrum of all materials.
- Module 4: A lateral track model has been implemented following the literature and a more complex one is still in progress. Both models rely on the decomposition of the rail into 3 beams to allow bending and torsion to be described at the same time. The first model is almost finished but a few corrections need to be implemented. The second model is still in development.
- Module 5: The noise emission calculation will be done via numerical integration to save time for the development of models in module 4.

Update on project modules, at the 2nd July 2019:

Modules	State	Comments
1		First set of measurements done, next one soon
2		-
3		-
4		1 model to correct, 1 model in dev.
5		Numerical integration to gain time
6		-
Reporting		6 months report written, next one for 9 months

Labels:

Done	In progress – On time	In progress - Delay

Update on project budget, at the 2nd July 2019:

Labels	Budget [CHF]
Salary 50% Post Doc – 9 months	38062.50
Sleeper Measurements Expert	4300
Project Management (5%) – 9 months	2439
Total	44801.50
Remaining from project budget	23500.50

VII - References

1. *Dynamical Mechanical Analysis, A beginner's guide*. PerkinElmer
2. *Mechanical vibration and shock - Characterization of the dynamic mechanical properties of visco-elastic materials – Time-Temperature superposition.* International Standard, ISO 18437-6, 2017.
3. *A new identification method of viscoelastic behavior: Application to the generalized Maxwell model.* F. Renaud, J.-L. Dion, G. Chevalier, I. Tawfiq, R. Lemaire. Mechanical Systems and Signal Processing, 25, 991-1010, 2011.
4. *Analyses of lateral vibration behaviour of railway track at high frequency using a continuously supported multiple beam model*. T.X. Wu and D.J. Thompson. Journal of the Acoustical Society of America, 106, 1369-1376, 1999.
5. *Railway Noise and Vibration: Mechanisms, Modelling and Means of Control*. D. J. Thompson, Elsevier 2008.